Hydrological Sciences Journal

ISSN: 0262-6667 (Print) 2150-3435 (Online) Journal homepage: http://www.tandfonline.com/loi/thsj20

Re-calibration of Arctic sea ice extent datasets using Arctic surface air temperature records

Ronan Connolly, Michael Connolly & Willie Soon

To cite this article: Ronan Connolly, Michael Connolly & Willie Soon (2017): Re-calibration of Arctic sea ice extent datasets using Arctic surface air temperature records, Hydrological Sciences Journal, DOI: 10.1080/02626667.2017.1324974

To link to this article: http://dx.doi.org/10.1080/02626667.2017.1324974

View supplementary material

Accepted author version posted online: 29 Apr 2017.
Published online: 22 May 2017.

Submit your article to this journal

Article views: 364

View related articles

View Crossmark data

Full Terms & Conditions of access and use can be found at
http://www.tandfonline.com/action/journalInformation?journalCode=thsj20

Download by: [131.142.188.56] **Date:** 02 June 2017, At: 07:44

HYDROLOGICAL SCIENCES JOURNAL – JOURNAL DES SCIENCES HYDROLOGIQUES, 2017
https://doi.org/10.1080/02626667.2017.1324974

Check for updates

Re-calibration of Arctic sea ice extent datasets using Arctic surface air temperature records

Ronan Connolly [a], Michael Connolly[a] and Willie Soon[b]

[a]Independent scientists, Dublin, Ireland; [b]Harvard-Smithsonian Center for Astrophysic Center for Astrophysics Solar, Stellar and Planetary Sciences Division, Cambridge, MA, USA

ABSTRACT

A new seasonal and annual dataset describing Arctic sea ice extents for 1901–2015 was constructed by individually re-calibrating sea ice data sources from the three Arctic regions (North American, Nordic and Siberian) using the corresponding surface air temperature trends for the pre-satellite era (1901–1978), so that the strong relationship between seasonal sea ice extent and surface air temperature observed for the satellite era (1979-present) also applies to the pre-satellite era. According to this new dataset, the recent period of Arctic sea ice retreat since the 1970s followed a period of sea ice growth after the mid-1940s, which in turn followed a period of sea ice retreat after the 1910s. Arctic sea ice is a key component of the Arctic hydrological cycle, through both its freshwater storage role and its influence on oceanic and atmospheric circulation. Therefore, these new insights have significance for our understanding of Arctic hydrology.

ARTICLE HISTORY
Received 9 October 2016
Accepted 13 January 2017

EDITOR
D. Koutsoyiannis

ASSOCIATE EDITOR
not assigned

KEYWORDS
Arctic sea ice; climate change; Arctic hydrological system; early 20th century warm period

1 Introduction

Satellite monitoring of Arctic sea ice has highlighted a dramatic decline in sea ice extent since at least the 1970s (e.g. Comiso *et al.* 2008, Cavalieri and Parkinson 2012, Meier *et al.* 2014). This decline has been observed for all seasons, although it is particularly pronounced for the month of September (i.e. late summer/early autumn). However, as the authors recently discussed in Soon *et al.* (2015), it is known that the Arctic warming since the 1970s followed a period of Arctic cooling from the 1940s, which in turn was preceded by an early 20th century warming (ETCW) period (e.g. Polyakov and Johnson 2000, Semenov and Bengtsson 2003, Bengtsson *et al.* 2004, Johannessen *et al.* 2004, Kuzmina *et al.* 2008, Brönnimann 2009, Bekryaev *et al.* 2010, Wood and Overland 2010, Yamanouchi 2011, Brönnimann *et al.* 2012, Hanna *et al.* 2012, Semenov and Latif 2012, Suo *et al.* 2013). There is also evidence that Arctic sea ice extents can vary substantially over multi-decadal to centennial time scales (e.g. Day *et al.* 2012, Miles *et al.* 2014). Therefore, in order to assess the significance of the satellite-era Arctic sea ice trends, it is important also to consider these trends in the context of the longer-term trends over the entire 20th century. For this reason, in this paper, we develop a new estimate of Arctic sea ice extent trends for the period, 1901–2015.

Because Arctic sea ice trends are closely correlated to Arctic temperature trends, they are often discussed in the context of global temperature trends, e.g. Meier *et al.* (2014). Meanwhile, in the past, the hydrological community tended to focus primarily on terrestrial and atmospheric hydrology, rather than sea ice and oceanic hydrology. However, it is important to remember that Arctic sea ice is also a key component of the Arctic hydrological cycle (e.g. Peterson *et al.* 2006) – see Figure 1.

As a component of the cryosphere[1] in the Northern Hemisphere, Arctic sea ice directly accounts for some of the freshwater stored in the Arctic Ocean, albeit in solid form. Recent estimates of its contribution to total freshwater storage vary from ~12% (Serreze *et al.* 2006, Haine *et al.* 2015) to ~18% (Aagaard and Carmack 1989) (see Table 1), which is not insignificant. Holland *et al.* (2007) even found the mean sea ice storage contribution of 10 different climate models to be 22%, although this result should be treated cautiously as the individual climate models gave widely different values. The rest of the freshwater is technically saline, but has a relatively low salinity, typically defined relative to a salinity of 34.8 (Aagaard and Carmack 1989, Serreze *et al.* 2006, Haine *et al.* 2015).

More importantly, because sea ice is a very dynamic component of the Arctic freshwater system, changes in sea ice extent are often one of the biggest

CONTACT Ronan Connolly ronanconnolly@yahoo.ie

[1]The cryosphere refers to the regions of the Earth where water is found in its solid form, e.g. ice or snow.

The supplementary material for this article can be accessed here.

© 2017 IAHS

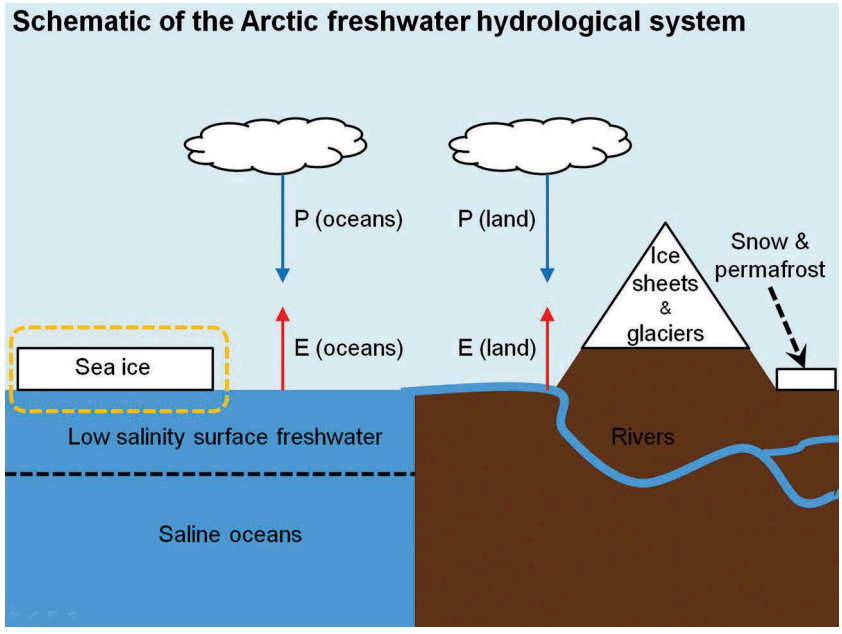

Figure 1. Schematic illustrating the main components of the Arctic hydrological system, including sea ice. P and E correspond to precipitation and evapotranspiration, respectively.

Table 1. Summary of various Arctic freshwater budget surveys estimating the mean freshwater storage of each of the components. Some addition of terms has been made to the original figures. Low salinity freshwater components are calculated relative to a salinity of 34.8. Missing components are indicated by dashes.

System	Phase	Aagaard and Carmack (1989): Observations		Serreze *et al.* (2006): Observations		Holland *et al.* (2007): mean of 10 climate models	
		km^3	%	km^3	%	km^3	%
Sea ice	Solid	17 300	18	10 000	12	13 851	22
Low salinity freshwater	Liquid	80 000	82	74 000	88	47 756	78
Ice sheets and glaciers	Solid	-	-	-	-	-	-
Rivers and lakes	Liquid	-	-	-	-	-	-
Snow and permafrost	Solid	-	-	-	-	-	-
Soil moisture	Liquid	-	-	-	-	-	-
Atmosphere	Mixed	-	-	140	0.2	-	-
Total		97 300	100	84 140	100	61 607	100

contributors to Arctic freshwater trends. For instance, Peterson *et al.* (2006) argued that there was a net freshening of the Arctic Ocean and seas over the 1960s–1990s period, and that ~50% of this freshening was due to sea ice melt (see Table 2).

Also, a major component of the annual transport of freshwater out of the Arctic Ocean is via sea ice export (Aagaard and Carmack 1989, Serreze *et al.* 2006, Dickson *et al.* 2007, Haine *et al.* 2015) (see Table 2) mainly through Fram Strait (Kwok *et al.* 2004), although transport through the Canadian Arctic Archipelago is also important (Haine *et al.* 2015, Münchow 2016). This general result of a major sea ice export component in Arctic freshwater transport has been replicated by climate models (Holland *et al.* 2006, 2007), although the exact contributions often differed widely between models (Holland *et al.* 2007).

Moreover, sea ice indirectly influences the other two key oceanic components of the Arctic hydrological system: net precipitation minus evapotranspiration ("P–E") and liquid freshwater transport. Sea ice acts as a regulator between evaporation and precipitation (Kopec *et al.* 2016), and current climate models predict that decreases in sea ice cover lead to increases in precipitation (e.g. Weatherly 2004, Deser *et al.* 2010, Bintanja and Selten 2014). Indeed, Kopec *et al.* (2016) have recently confirmed that precipitation rates in the Arctic are directly linked to Arctic sea ice extent (Wake 2016).

The liquid freshwater component of the Arctic Ocean (technically the freshwater component of low-salinity water) is also strongly influenced by the presence or absence of sea ice. That is, the melting of sea ice leads to the formation of a low-salinity meltwater layer, while the growth of sea ice increases the salinity of the water underneath (Rudels 2016).

Table 2. Estimates of Arctic freshwater transport components of the Arctic hydrological system. Some summation of terms has been carried out to the original figures. Dashes indicate components missing from budgets. 10^6 m^3/s = 1 sverdrup (Sv) = 31 536 km^3/year. P–E refers to net precipitation minus evapotranspiration.

	Unit	Sea ice melt	Sea ice export	Freshwater transport	Glacial melt	River runoff	Snow /permafrost	P–E, oceans	P–E, land	Total
Peterson *et al.* (2006):	km^3/year	817	-	-	119	104	-	608	-	1648
Observations	(%)	50	-	-	7	6	-	37	-	100
Aagaard and Carmack (1989):	km^3/year	-	−2790	−520	-	3300	-	900	-	890
Observations	(%)	-	−313	−58	-	371	-	101	-	100
Serreze *et al.* (2006):	km^3/year	-	−2460	−3450	-	3200	-	2000	2900	2190
Observations	(%)	-	−112	−158	-	146	-	91	132	100
Dickson *et al.* (2007): Arctic to	10^6 m^3/s	-	−0.088	0.127	0.009	0.102	-	0.065	-	0.215
Atlantic flux	(%)	-	−41	59	4	47	-	30	-	100
Holland *et al.* (2006): CCSM climate model	10^6 m^3/s	-	−0.104	−0.09	-	0.115	-	0.057	-	−0.02
Holland *et al.* (2007): 10 climate	km^3/year	-	−1841	−1388	-	3162	-	1543	3162	4638
models	(%)	-	−40	−30	-	68	-	33	68	100

Finally, Arctic sea ice extent seems to play an important role in mid-latitude weather via its influence on atmospheric and oceanic circulation patterns (e.g. Aagaard and Carmack 1989, Francis *et al.* 2009, Cohen *et al.* 2014, Vihma 2014, Overland *et al.* 2015). Therefore, Arctic sea ice is also of relevance for mid-latitude precipitation patterns (Vihma 2014). For instance, the East Asian summer monsoon seems to be strongly influenced by the spring Arctic sea ice extent (Guo *et al.* 2014) and Liu *et al.* (2012) have found that autumn Arctic sea ice area influences winter snowfall in Europe and the United States.

For these reasons, accurate estimates of medium-to-long-term Arctic sea ice extent trends are of particular importance for studying Arctic hydrological trends. However, the widely used satellite-derived sea ice estimates only cover the post-1970s period. Therefore, developing a reliable long-term Arctic sea ice dataset that includes the pre-satellite era would be of considerable value for improving our understanding of Arctic hydrology.

Although there are several useful sea ice datasets predating the satellite era, such as the "Walsh" (Walsh and Johnson 1979, Walsh and Chapman 2001, Walsh *et al.* 2015, 2017), "Vinje" (Vinje 2001, ACSYS 2003, Divine and Dick 2006) and "Zakharov" (Zakharov 1997, Polyakov *et al.* 2003, Mahoney 2008, Frolov *et al.* 2009) datasets, these pre-satellite estimates were constructed from different data sources for different periods. For instance, for the 1920s–1930s, data are mostly limited to occasional observations from ships, airplanes and weather stations, while for the 1950s–1970s, data from drifting buoys as well as more regular ship- and air-based observations are also available.

Moreover, in some cases there is no overlap between individual data sources. For example, single-channel passive microwave satellite measurements from NIMBUS-5 were recorded from late 1972 until early 1977, providing some useful satellite data for the mid-1970s. However, the current multi-channel passive microwave satellite-derived estimates did not begin until October 1978 (Cavalieri *et al.* 1984). This lack of overlap prevents a direct *simultaneous* comparison between the two datasets. So, while some studies have compared and contrasted the different trends of the two sets of satellite data (e.g. Parkinson and Cavalieri 1989, Meier *et al.* 2012), most analyses of the satellite era begin in 1978 (e.g. Comiso *et al.* 2008, Cavalieri and Parkinson 2012, Meier *et al.* 2014).

Prior to the satellite era, geopolitical considerations were also a problem for the compilers of datasets. In particular, during the Cold War, data sharing between the Soviet Union and western Arctic nations was almost non-existent. As a result, for the pre-satellite era, the American-based Walsh group had very few observations for the Russian Arctic, and in their dataset most of the estimates for these regions were based on (often crude) extrapolations and inferences. For this reason, while their dataset nominally describes the entire Arctic Ocean and seas before the satellite era (and especially pre-1953), it is probably better considered as an estimate for the North American and Nordic Arctic. It is worth noting that the Walsh dataset is the primary pre-1972 data source for the Hadley Centre's popular HadISST dataset (Rayner *et al.* 2003, Titchner and Rayner 2014). On the other hand, the Russian-based Zakharov group had very few observations for the North American Arctic, and as a result, their datasets only consider the Russian and Nordic regions. However, since the publication of Mahoney (2008), both datasets are now publicly available. So, in this paper, we will combine the Russian dataset with the western datasets, to provide a new pan-Arctic estimate for the pre-satellite era. At the time of writing, an update to the Walsh dataset was in preparation, which apparently will include the Russian dataset (Walsh *et al.* 2015, 2017). We note that while we

were writing this paper, Pirón and Pasalodos (2016) also independently decided to combine these two datasets for their reconstruction of September sea ice extents.

The above inconsistencies introduce considerable challenges into attempts to composite all of the multiple data sources into a single sea ice extent index spanning the period since the early 20th century. However, the decline in Arctic sea ice extent during the satellite era coincided with a corresponding increase in the average surface air temperatures for the Arctic. This is consistent with a strong relationship between Arctic sea ice extent and Arctic surface air temperatures, suggesting that Arctic surface air temperature trends can be used as an indirect proxy for calibrating Arctic sea ice trends, particularly for the Arctic summer (Alekseev *et al.* 2016).

Indeed, Alekseev *et al.* (2016) recently used Arctic summer surface air temperatures as a direct (inverse) proxy for September Arctic sea ice extent by applying a simple linear regression relationship. Alekseev *et al.*'s approach bypasses the problems from the multiple data sources described above. It therefore offers a useful approximate estimate of Arctic September sea ice extent trends for the 1900–2013 period. However, because the Alekseev *et al.* (2016) reconstruction is essentially an inverse Arctic summer temperature index, it cannot be used for studying the relationship between Arctic sea ice extent and surface air temperatures outside the satellite era (as that would lead to circular logic). Also, it discards all of the pre-satellite era direct observations of Arctic sea ice incorporated in the Walsh and Zakharov datasets.

Another related approach is to use climate models forced with prescribed empirical temperature data to evaluate sea ice data or *vice versa* (e.g. Brönniman *et al.* 2008, Kauker *et al.* 2008, Semenov and Latif 2012, Semenov 2014). For instance, Kauker *et al.* (2008) used the sea ice component of a climate model to estimate how the sea ice extents should have varied over the 1900–1997 period given the observed Arctic meteorological conditions (mainly in terms of surface air temperatures and sea level pressures) over that period. Most of their simulated sea ice reconstructions showed similarities with the Zakharov dataset and others. This offers further evidence that the sea ice–temperature relationship probably also applied during the pre-satellite era.

With that in mind, in this paper, we take an intermediate approach which preserves useful information provided by the pre-satellite era Arctic sea ice datasets, but also uses information from Arctic surface air temperature trends to reduce the problems arising from changes in data sources. Specifically, we first divide the Arctic Ocean into three separate regions: North American Arctic, Nordic Arctic and Siberian Arctic. We then use the seasonal relationships for each of these regions between Arctic surface air temperatures and sea ice extents during the satellite era as a baseline. This baseline is then used to re-calibrate each of the individual components of the pre- and post-satellite era sea ice extent measurements. These re-calibrated components are then composited together to construct seasonal sea ice extent indices for each of the three regions. These regional estimates are then used to construct new annual and seasonal Arctic sea ice extent indices from 1901 to 2015. Because much of the pre-satellite era data is quite limited, we confine our analysis specifically to sea ice *extents* and therefore do not consider some of the more detailed sea ice observations that have become possible in recent years, such as sea ice thickness or volume (e.g. Tilling *et al.* 2015).

2 Arctic region definitions

For the purposes of this study, we divide the Arctic Ocean and Seas into three different regions (see Fig. 2). These geographic areas are the North American Arctic, the Nordic Arctic and the Siberian Arctic. In keeping with the International Hydrographic Organization (IHO) *Names and Limits of Oceans and Seas* (International Hydrographic Organization 2002), all of the seas considered have a lower latitude limit of at least 60°N, with the exception of Hudson Bay and Hudson Strait (both of which have a southern limit below 60°N). Therefore, our analysis does *not* consider some of the lower latitude seas in the Northern Hemisphere with winter sea ice, e.g. the Bering Sea, the Sea of Okhotsk, the Gulf of St Lawrence and the Baltic Sea. Seasonal sea ice in these non-Arctic seas is shown in white in Figure 2.

There are useful datasets that provide some information about sea ice coverage in the pre-satellite era for some of these seasonal sea ice regions. For instance, Mahoney *et al.* (2011) compiled sea ice observations for the Bering Sea (and Chukchi Sea) from the logbooks and journals of whaleships, and Hill *et al.* (2002) compiled a similar dataset for the Gulf of St Lawrence and Nova Scotia from a variety of data sources. This raises the possibility that our analysis could also be extended to incorporate the non-Arctic regions of the Northern Hemisphere where seasonal sea ice can occur. Apparently, the new version of the Walsh dataset, which was in preparation at the time of writing, will incorporate these non-Arctic datasets (Walsh *et al.* 2015). However, it can be seen from Figure 2 that the three Arctic regions encompass most of the sea ice extent at the peak of the Arctic winter (~80–82% in March) and

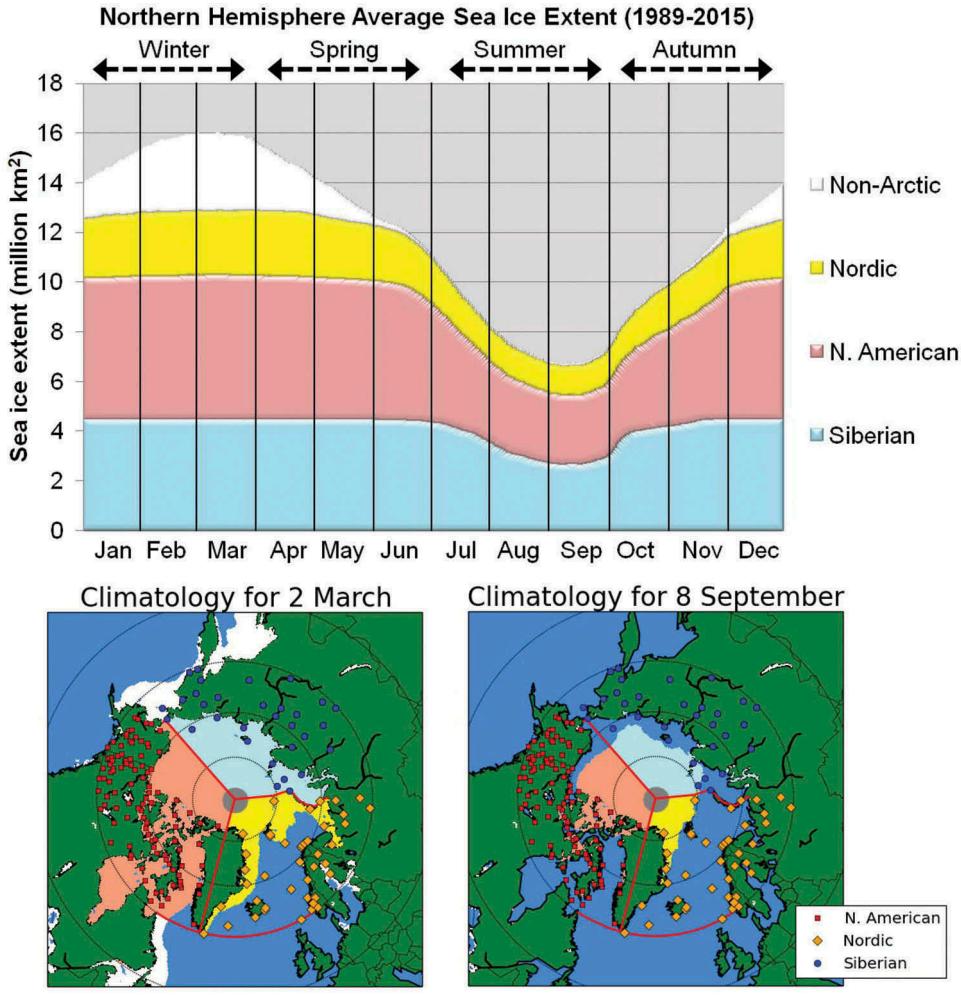

Figure 2. Mean Northern Hemisphere sea ice extents over the period 1989–2015, as derived from the DMSP satellite measurements. Each of the three Arctic regions are outlined with solid red lines, and the ice extents within these regions are shaded with different colours. The locations of the rural stations used for determining surface air temperature trends for these regions are also shown.

almost all of the extent during the Arctic summer (~98–99% in September). Therefore, for this study, we confine our analysis to the Arctic Ocean and seas.

We can see from Figure 2 that the minimum Arctic sea ice extent for all regions occurs in early September and the maximum extent occurs in early March. For this reason, when describing the Arctic seasons, it is common to define winter as January, February and March; spring as April, May and June; summer as July, August and September; and autumn as October, November and December. For consistency with previous studies (e.g. Zakharov 1997, Walsh and Chapman 2001), we will also use these definitions.

These Arctic season definitions are often surprising to those unfamiliar with the Arctic sea ice climatology, since we are used to the Northern Hemisphere seasons being defined, for example, in terms of the winter solstice (21 December) and summer solstice (21 June). However, in the Arctic, the regimes of sea ice growth and melt play a more dominant role in defining seasonality than at lower latitudes. These regimes are influenced by factors such as the feedback between sea ice coverage and albedo (e.g. Curry *et al.* 1995, Perovich and Polashenski 2012). That is, as the amount of incoming sunlight increases during the summer, melting the sea ice, the surface albedo is reduced, meaning more sunlight is absorbed, which melts the sea ice further. Due to factors such as this, the peaks and troughs in sea ice extent lag the corresponding peaks and troughs in day length by ~3 months (Zakharov 1997).

3 Data and methods

Aside from a small blind-spot at the poles, arising from the orbital paths of the satellites involved, the passive microwave satellite-derived sea ice estimates provide almost complete geographical coverage (Cavalieri

et al. 1984, 1996, Maslanik and Stroeve 1999, Ivanova *et al.* 2015). They also provide measurements quite frequently, being daily since 1987 (albeit with a 2 month gap during December 1987 and January 1988). Therefore, we can have relatively high confidence in our estimates of total and regional sea ice extents during the satellite era.

Unfortunately, as discussed above, the available sea ice observations for most of the pre-satellite era (i.e. before the 1970s) are quite limited both spatially and temporally. As a result, the actual sea ice conditions for many regions of the Arctic were not observed by the various monitoring groups. Additionally, the observation methods and practices used by each of the groups varied substantially over the years – generally improving over time.

This means that the uncertainty associated with total sea ice estimates increases dramatically the further back in time we go back. However, ironically, the annual and seasonal variability *implied* by the observations is reduced for these earlier years because the data coverage is so much more limited. This could have led to an underestimation of sea ice variability in the pre-satellite era (particularly for the earlier decades), potentially introducing a coverage bias into the pre-satellite era trends. This is analogous to the underestimation of early-to-mid 20th century hurricane frequencies, which seems to have occurred before the installation of systematic hurricane detecting networks (e.g. Landsea *et al.* 2008).

In this paper, we attempted to reduce the magnitude of these problems with the pre-satellite data by using the observed relationships between Arctic surface air temperatures and Arctic sea ice extent (e.g. Zakharov 1997, Alekseev *et al.* 2016). Specifically, we determined the relationships between surface air temperatures and sea ice extent for each of the seasons and regions during the satellite era, using linear least-squares fits.

We explicitly assumed that these relationships would have been (at least broadly) similar during the pre-satellite era. Therefore, like Alekseev *et al.* (2016), we used these relationships to convert our regional and seasonal temperature reconstructions into proxies for the corresponding sea ice extents. However, these sea ice extent proxies do not contain any of the information from the actual pre-satellite era sea ice observations. So, unlike Alekseev *et al.* (2016), we only used these proxies as an additional dataset for recalibrating the pre-satellite era datasets, or when direct observations are unavailable.

For a given region, we split up the available pre-satellite datasets into different periods, corresponding to the major changes in data sources. For instance, for the Walsh dataset (Section 3.3), the 1953–1971 period was analysed separately from the pre-1953 periods, since it has much greater spatial coverage (Walsh and Johnson 1979, Walsh and Chapman 2001, Walsh *et al.* 2015, 2017).

For each of the seasons, regions and periods, we rescaled the data series so that its mean and standard deviation were the same as those for our temperature-derived sea ice extent proxy for the corresponding season, region and period. This has similarities to the approach used by Meier *et al.* (2012) to recalibrate 1953–1977 pre-satellite and early satellite data to be more consistent with the 1978–2011 satellite data. Each of these rescaled components was then composited to provide regional and seasonal estimates for the entire 1901–2015 period. The regional estimates were then composited to give seasonal estimates for the entire Arctic region.

Most of the gridded datasets we analysed in this paper use slightly different formats and data types. So, for each of the gridded datasets, we wrote separate scripts using the Python programming language (https://www.python.org/) to calculate the relevant seasonal data series for each of the Arctic regions. These seasonal data series were then analysed, re-calibrated and composited with the non-gridded datasets using a popular spreadsheet package (MS Excel, https://products.office.com/en/excel). These data series, along with our final re-calibrated sea ice extent indices, are provided in the Supplementary Information. Additionally, the Python scripts and further output files from the analysis are archived on the FigShare website at https://doi.org/10.6084/m9.figshare.4879565.v3.

In the rest of this section, we briefly discuss the different datasets we used for this analysis.

3.1 Surface air temperature data (1900–2015)

The source we used for determining surface air temperature trends was version 3 of the Global Historical Climatology Network (GHCN) monthly dataset, which was downloaded from http://www.ncdc.noaa.gov/ghcnm/*[Accessed 11 January 2016]*. This dataset of monthly averaged weather station temperature records is compiled and maintained by the US-based NOAA National Centers for Environmental Information (Lawrimore *et al.* 2011). They provide two versions of the dataset. The first dataset contains the raw monthly station records with only some minor quality control adjustments, but the records for the second dataset have been adjusted by the automated homogenization algorithm of Menne and Williams (2009) in an attempt to remove/reduce any non-climatic biases that may exist in the raw station records. We refer to the former as the "unadjusted dataset" and the latter as the "MW09-adjusted dataset".

From Figure 3, we can see that the long-term temperature trends for the Arctic region are quite similar for both the unadjusted and the MW09-adjusted datasets. That is, both datasets imply that the Arctic went through a period of warming (~1900s–1940s), followed by a period of cooling (~1940s–1970s), followed by another period of warming (~1970s–present). As discussed in the introduction, the existence of this alternation between warming and cooling periods for the Arctic over the 20th century has been well documented. The available temperature records suggest that 19th century Arctic temperatures were cooler than for the 20th century (Przybylak *et al.* 2010); however the data available for this earlier period are very limited and for this paper we stick to the period from 1901 to the present.

The net effect of the MW09-adjustments is to slightly reduce the apparent warmth of *both* the present warm period and the early 20th century warm period, and so the relative warmth of both warm periods is comparable for both datasets. Also, the timing of the warming and cooling periods is the same. Therefore, the results of our analysis should be quite similar, regardless of which dataset we used. In this paper, we used the unadjusted dataset. However, for interested readers, the equivalent analysis using the MW09-adjusted dataset is also provided in the Supplementary Information.

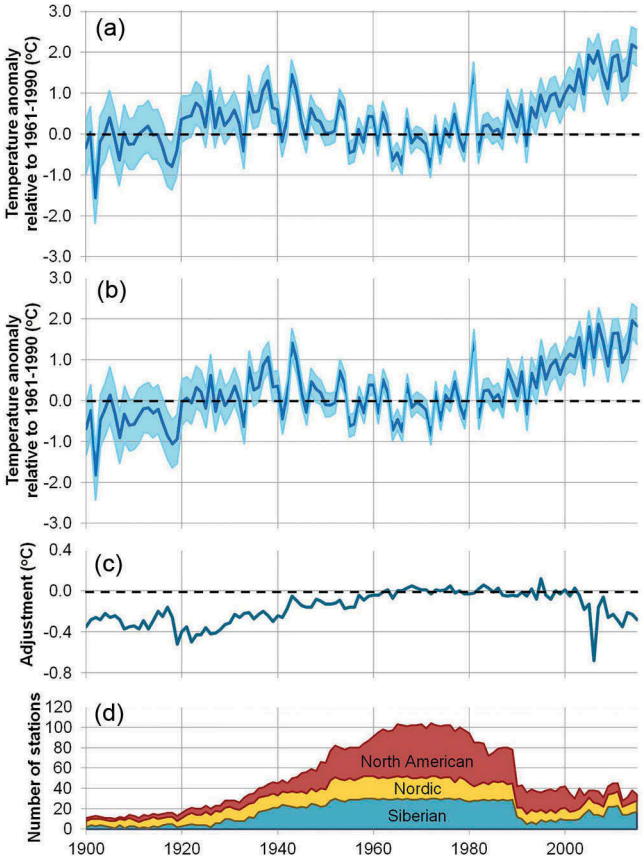

Figure 3. Annual temperature trends for the entire Arctic region according to the (a) unadjusted and (b) MW09-adjusted datasets; (c) the net effect of the MW09 adjustments on Arctic temperature trends; and (d) the numbers of stations in the datasets with data for each year. Error bar envelope refers to twice the standard error.

The procedure we used for determining the regional temperature trends from the GHCN dataset is essentially the same one we used in Soon *et al.* (2015), and the details are described there (and references therein). However, for our Arctic region in Soon *et al.* (2015), we limited our analysis strictly to those stations within the "Arctic Circle", i.e. those north of 66°33′N. This meant we could use only 77 stations. For this paper, we are using a less restrictive definition for the Arctic (see Section 2), since the average Arctic sea ice extent covers a wider region than just the Arctic Circle. Therefore, for this analysis, Arctic stations are defined as those north of 60°N.

As we noted in Soon *et al.* (2015), while the Arctic is a relatively unpopulated region and is therefore generally unaffected by urbanization, weather stations tend to be near/in human settlements. Hence, urbanization bias can still occur for Arctic weather stations, e.g. Hinkel and Nelson (2007), Konstantinov *et al.* (2015). Because we were restricted by the shortage of Arctic Circle stations, some of the stations (23%) we used for Soon *et al.* (2015) showed at least some signs of urbanization, and so it is plausible that urbanization bias might have slightly contributed to the trends for that region. However, as the analysis in this paper covers a wider area than just the Arctic Circle, there are more stations available. Therefore, we only used GHCN stations that are "fully rural", i.e. rural in terms of both associated population and night-light intensity; see Soon *et al.* (2015) for a discussion.

3.2 Satellite-derived Arctic sea ice extent data (1978–2015)

For our satellite-era estimates of sea ice extents, we used the NASA Team's gridded datasets (Cavalieri *et al.* 1996, Maslanik and Stroeve 1999), which we downloaded from the National Snow and Ice Data Center (NSIDC) website, https://nsidc.org/*[Accessed 14 January 2016]*. Together, these datasets cover the period, October 1978 to present. Using a Python script, we used these datasets to calculate the average seasonal sea ice extent in each year for each of our Arctic regions.

We should note that the 1978–present satellite record is actually a composite of several different satellites, i.e. Nimbus-7, DMSP-F8, DMSP-F11, DMSP-F13 and DMSP-F17 (Cavalieri *et al.* 1996, Maslanik and Stroeve

1999). Each of these satellites had slightly different sensors, orbits, calibrations, etc., and only operated for a decade or so. So, it is plausible that some of the apparent long-term trends in the satellite estimates could be a consequence of the changes in satellites. However, aside from a 2-month gap in late 1987, there was usually a short overlap between the end of one satellite mission and the beginning of the next. This means that Cavalieri *et al.* were able to use these overlapping periods to recalibrate the data from each of the individual satellites to provide a reasonably consistent dataset (Cavalieri *et al.* 1996, Maslanik and Stroeve 1999).

It is important to stress that microwave satellite-derived estimates of sea ice concentrations are *not* based on actual observations of sea ice conditions, as might be initially assumed. Rather, the sea ice concentrations in a given area are inferred from the spectral properties of the microwave emissions from that area during the satellite's orbit, using an automated computer algorithm (e.g. Cavalieri *et al.* 1984, Ivanova *et al.* 2015). These algorithms typically try to distinguish between the microwave emissions from open water, land, sea ice and different categories of sea ice (e.g. multi-year sea ice versus newly formed sea ice) by comparing the emissions at different microwave frequencies, although these comparisons are not possible for the earlier NIMBUS-5 satellite (1972–1977), which had only a single-channel passive microwave detector. However, although these automated algorithms are generally quite accurate, they are not perfect and sometimes provide misleading artefacts which direct visual observations would avoid. For instance, the microwave emissions from open water are very hard to distinguish from temporary melt-water pools on the surface of sea ice sheets. For this reason, the microwave satellite estimates tend to underestimate the total sea ice area when there are a lot of melt-water pools, which is particularly common during the Arctic summer (e.g. Cavalieri *et al.* 1984, Ivanova *et al.* 2015).

If these artefacts of the automated algorithms lead to a systematic underestimation of the total Arctic sea ice extents, but it is by a similar amount every year, then this should not be a major problem for our analysis, since our pre-satellite estimates will be rescaled as part of our reconstruction. However, suppose the relative fraction of melt-water pools increases during relatively warm periods (for instance). In that case, it is plausible that the satellite estimates could potentially exaggerate the rate of melting during the recent Arctic warming relative to terrestrial observations. This introduces a potential problem in comparing the satellite-era estimates with pre-satellite observations during earlier periods of Arctic warming, such as the 1920s–1940s. However, for our analysis in this paper, we explicitly assume that these satellite-derived estimates are reasonably accurate. This is supported by the reasonable agreement with the other sea ice datasets and the surface air Arctic temperature trends during the 1978–2015 period.

Moreover, although the satellite-derived estimates are sometimes less accurate than direct visual observations would be, they provide nearly complete geographical coverage (except for the orbital "blind-spot" near the poles). For this reason, the satellite-derived estimates of total and regional sea ice extents are probably more consistent and reliable than those from the pre-satellite era, which were derived from spatially incomplete and intermittent observations.

There is considerable debate over which of the various algorithms is most reliable for estimating sea ice concentrations, e.g. see Ivanova *et al.* (2015) for a comparison of the main algorithms. However, the long-term trends implied by all of the current algorithms during the satellite era are broadly similar. The algorithm used for the NASA Team's satellite datasets used in this paper was described in Cavalieri *et al.* (1984).

In this paper, we define the seasonal sea ice "extent" as the total area of those gridboxes with a mean sea ice concentration of at least 15% for that season. The mean seasonal sea ice extents for each of the regions over the satellite era are plotted in Figure 4.

Although the North American and Siberian Arctic together account for most of the sea ice extent, for both of these regions there has been very little variability in sea ice extent in the winter, spring or autumn. Instead, almost all of the variability in sea ice extent for these regions has occurred during the summer season (although there was some variability for the North American Arctic during the autumn). Therefore, most of the variability in Arctic sea ice extent during the winter and spring (and to a lesser extent the autumn) occurred in the Nordic Arctic. This is in keeping with the analysis in Section 2. On the other hand, during the summer season, all three Arctic regions showed a general decrease in sea ice extent over the satellite era (1979–2015), as has been noted elsewhere (e.g. Comiso *et al.* 2008, Cavalieri and Parkinson 2012, Meier *et al.* 2014).

3.3 The "Walsh" sea ice dataset (1901–2011)

At the time of writing, the most widely used estimates for Arctic sea ice extents during the pre-satellite era are the so-called "Walsh dataset" developed by Walsh *et al.* (Walsh and Johnson 1979, Walsh and Chapman 2001, Walsh *et al.* 2015, 2017), and the Hadley Centre's HadISST dataset (see Section 3.5), which is based on the Walsh dataset. Version 1 of the Walsh dataset was

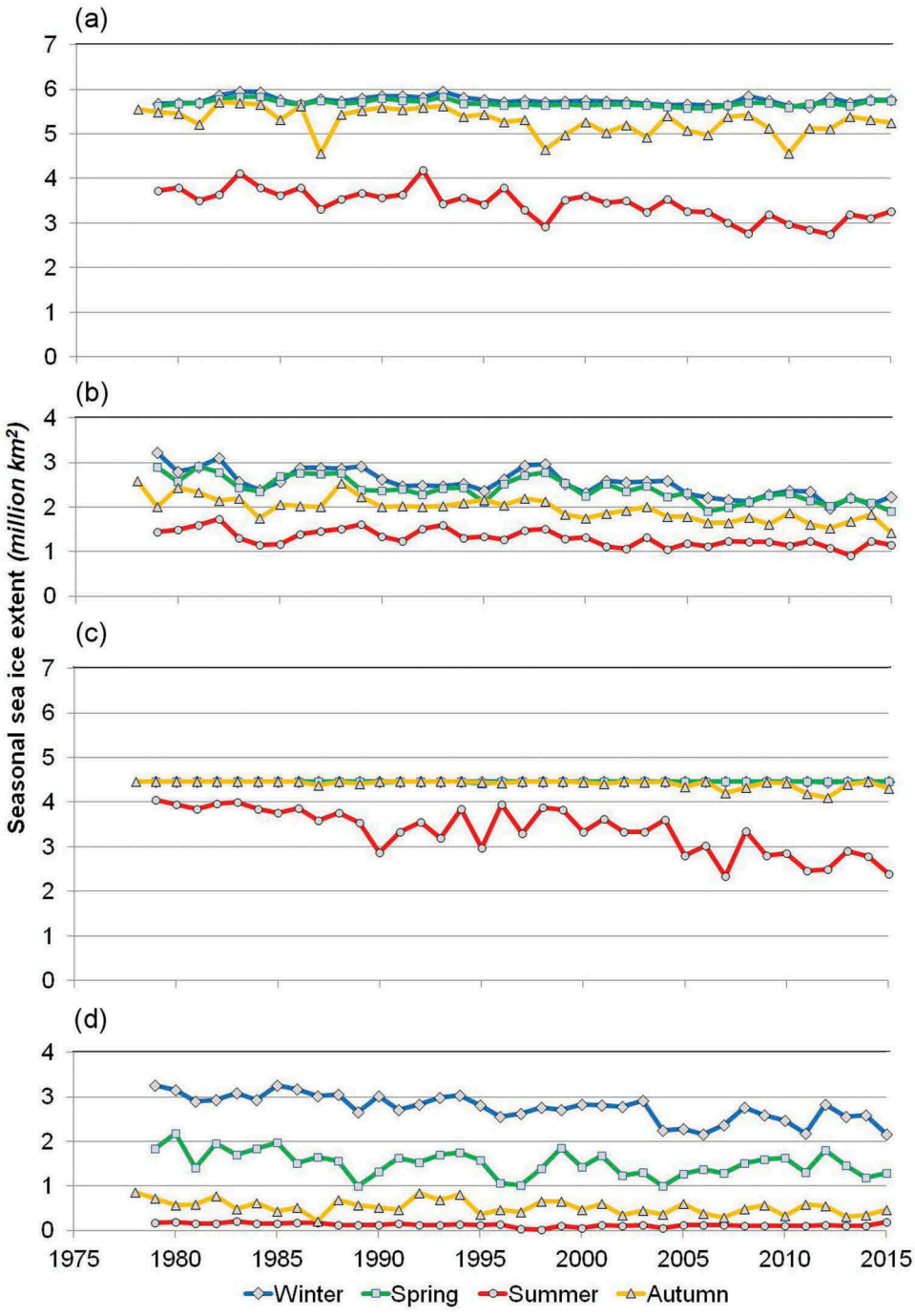

Figure 4. Mean seasonal sea ice extents (in million km^2) for each of the regions during the satellite era: (a) North American Arctic, (b) Nordic Arctic, (c) Siberian Arctic, (d) Non-Arctic.

one of our main sources for pre-satellite ice extents, which we downloaded from http://arctic.atmos.uiuc.edu/SEAICE/*[Accessed 12 January 2016]*.

Sea ice concentrations in the Walsh dataset are only reported to the nearest 10%, which is a problem since the standard definition of sea ice extent that we use for this study is a sea ice concentration of at least 15%. However, when calculating the average seasonal extents, we calculated the sea ice concentrations for each grid box (to the nearest 10%) for all three months. If the average concentration over the 3-month period was greater than 15%, then that grid box was treated as being within the sea ice extent for that year.

Up until 1953, the spring and summer estimates in the Walsh dataset are predominantly based on Arctic sea ice charts compiled by the Danish Meteorological Institute (DMI) (Danish Meteorological Institute (DMI), and NSIDC 2012) and digitized by Kelly

(1979). For the autumn and winter estimates for the pre-1953 period, Walsh and Chapman (2001) relied primarily on ship reports, which were also provided by the DMI. Separately, Vinje *et al.* (Vinje 2001, ACSYS 2003, Divine and Dick 2006) compiled estimates of the sea-ice edges[2] for the Nordic Seas with some observations dating back to 1553. Walsh and Chapman (2001) also used this Vinje dataset in their estimates for the Nordic Seas.

Figure 5(a) provides a typical example of one of the DMI sea ice charts (from August 1952). While these sea ice charts nominally provide estimates for the entire Arctic region, it is striking how sparse the regions where estimates were derived from actual observations (coloured in red) are. Most of the observations the DMI chart compilers had were from the Nordic Arctic and to a lesser extent the Canadian Arctic. Particularly during the Cold War, the DMI had very few observations for the Russian Arctic and most of their estimates for this region were described by the compilers as "*ice supposed but no information at hand*". Therefore, since these DMI charts are the primary pre-1953 data source for the Walsh dataset, the pre-1953 estimates for the Russian Arctic (in particular) should be treated with considerable caution.

3.4 The "Russian" sea ice datasets (1900–2008)

As discussed above, the pre-satellite era portion of the Walsh dataset contains very little information for the Russian Arctic region east of the Barents Sea, namely the Kara, Laptev, East Siberian and western Chukchi Seas. On the other hand, these are regions that were routinely monitored by Russian researchers, particularly in the second half of the 20th century. In 2007, in conjunction with the US-based NSIDC, the Russian-based Arctic and Antarctic Research Institute (AARI) digitized and published several datasets based on these data (Arctic and Antarctic Research Institute (AARI) 2007, Mahoney 2008, Mahoney *et al.* 2008, Frolov *et al.* 2009). Much of the analysis by Zakharov (1997) was based on an earlier version of this dataset. Mahoney *et al.* (2008) specifically noted that these Russian data had not been incorporated into the Walsh dataset, or

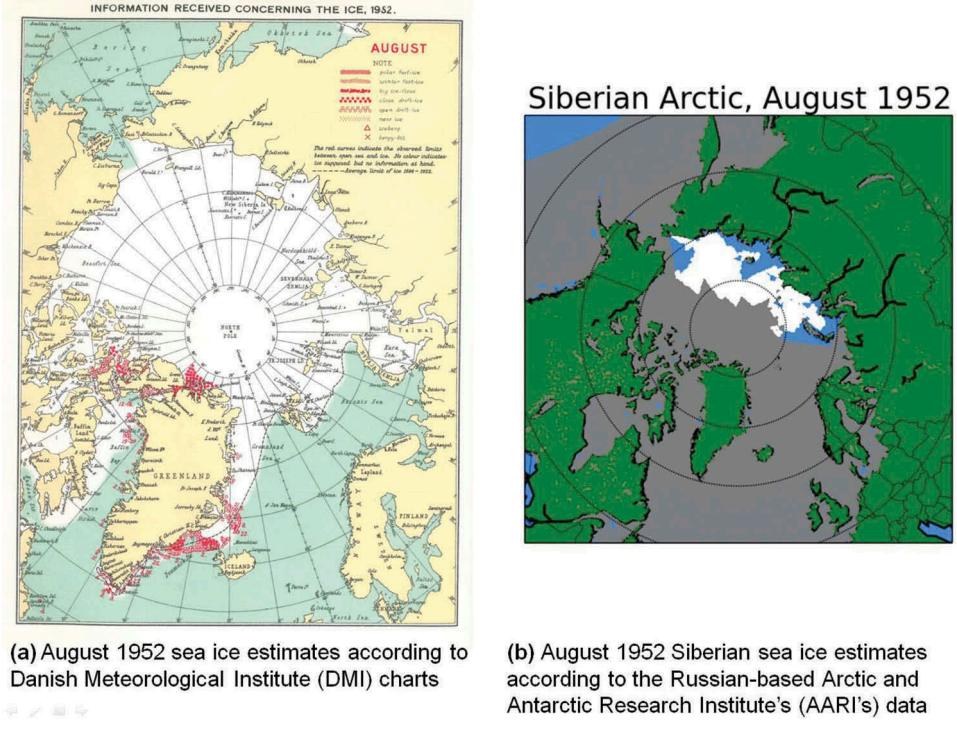

(a) August 1952 sea ice estimates according to Danish Meteorological Institute (DMI) charts

(b) August 1952 Siberian sea ice estimates according to the Russian-based Arctic and Antarctic Research Institute's (AARI's) data

Figure 5. (a) Example of one of the Danish Meteorological Institute sea ice charts (August 1952) used by Walsh and Chapman. The estimates coloured in red are derived from actual observations. The compilers did not have any observations for the white regions, but supposed there might have been ice there. Image courtesy of the Danish Meteorological Institute and the National Snow and Ice Data Center, University of Colorado, Boulder (Danish Meteorological Institute (DMI), and NSIDC 2012). (b) Example of observations from the Russian-based AARI dataset: average sea ice extent for the same month (August 1952).

[2]Although the sea ice *edge* is not the exact same as the sea ice *extent*, both metrics are related, and so these data can be used for estimating sea ice extents (and concentrations).

the related HadISST dataset, and they recommended that they should be included in future historical datasets of Arctic sea ice. In this study, we follow this recommendation. While we were preparing this paper, Pirón and Pasalodos (2016) independently developed a new Arctic sea ice dataset, which also followed this recommendation; and apparently an update to the Walsh dataset is in preparation, which will also incorporate the Russian dataset (Walsh *et al.* 2015, 2017).

One of the AARI datasets consists of a digitized compilation of Russian sea ice charts for the period 1933–2006 (Arctic and Antarctic Research Institute (AARI) 2007) with a gap during the period 1993–1996. These sea ice charts cover various parts of the Siberian Arctic, namely the Barents, Kara, Laptev, East Siberian and western Chukchi Seas (see Fig. 5(b)).

It is worth directly comparing Figure 5(a) and (b), since both of these maps describe the sea ice extent for the exact same month and year (August 1952), but using different data sources. While the AARI estimates (Fig. 5 (b)) only describe the regions for which the AARI had observations (i.e. part of the Russian Arctic), the DMI sea ice charts (Fig. 5(a)) nominally describe the entire Arctic, including the Russian Arctic. However, when the DMI charts were being compiled, the compilers did not have any actual observations for most of the regions they were considering. As a result, for many regions (especially the Russian Arctic), their estimates for a given month are often little more than guesses.

Indeed, we can see that all of the regions in Figure 5 (b) that the AARI directly observed to be ice free in August 1952 were incorrectly assumed (without any observations) to be ice packed in the corresponding DMI chart. For this reason, the "supposed ice" regions in the DMI charts (the primary pre-1953 data source for the Walsh dataset) should be treated sceptically. Therefore, we used the AARI datasets as our primary source for the pre-satellite era Russian Arctic.

Although there are some Russian sea ice data for the early 20th century (Frolov *et al.* 2009), systematic observations by the AARI did not begin until about 1933, following the decision by Russia during the Second International Polar Year in 1932 to develop the Northern Sea Route as a regular transport route (Mahoney *et al.* 2008).

For the earlier part of the 1933–2006 record, the charts were derived from systematic aircraft reconnaissance 1–3 times per month, along with ship and coastal observations. However, from 1953–1972, these were supplemented by observations from a network of drifting buoys and, beginning in the late 1960s, satellite observations (Mahoney *et al.* 2008). The first satellite observations (1966–present) used instruments that analysed the visible range, but later satellites (1972–present) were also able to monitor infrared frequencies.

Initially, aerial reconnaissance was limited mostly to the summer months and the spatial coverage did not extend far into the central Arctic (Mahoney *et al.* 2008). However, the coverage generally improved over time. Also, while the earlier aerial reconnaissance was based only on visual observations, from 1951–1992, aerial photography and other instrumented observations were also incorporated.

Although the AARI sea ice charts do not provide complete spatial coverage for the Russian Arctic(especially for the earlier years), Mahoney *et al.* (2008) and Mahoney (2008) developed an automated algorithm to estimate the average monthly and seasonal ice extents for each of the Russian Seas, when and where observations were available. This dataset was our primary source for sea ice extents in the Siberian Arctic for the period 1933–2006. It was downloaded from http://nsidc.org/*[Accessed 16th January 2016]*(Mahoney 2008).

For some years (particularly in the earlier period), Mahoney *et al.* (2008) and Mahoney (2008) did not have seasonal estimates for all four of the Siberian seas, namely the Kara, Laptev, East Siberian and western Chukchi. However, as discussed in the Supplementary Information, the average sea ice extent for each of the four seas is closely related to the total Siberian Arctic sea ice extent for a given season. With this in mind, for those years when we did not have data for all four seas in a given season, we estimated the total Siberian sea ice extent by extrapolation from those seas that did have data.

Additionally, Frolov *et al.* (2009) combined the more systematic AARI sea ice charts with a variety of other sources containing descriptions of early Arctic voyages and other observations to develop an extended reconstruction of August (i.e. mid-summer) sea ice extents for the Nordic and Siberian regions, covering the period 1900–2008. Their reconstruction also estimated April (i.e. end-of-winter) sea ice extents for the Nordic region (i.e. the Greenland and Barents Seas). We used this dataset to extend our Siberian analysis to include the 1901–1933 period. However, it is important to stress that the data these pre-1933 estimates were derived from are rather limited, and should be treated with particular caution.

As with the Mahoney *et al.* datasets, the Frolov *et al.* Siberian reconstruction provided estimates for each of the four Siberian seas. However, while the Mahoney *et al.* datasets nominally included the Siberian region of the Arctic Ocean north of these four seas, the Frolov *et al.* estimates did not. This extra region covers approximately 1 952 000 km^2, which is ~44% of the

Siberian Arctic region. However, this region is almost entirely ice packed even during the summer. Therefore, for the 1900–1933 period of our analysis when we used the Frolov *et al.* dataset, we added 1 952 000 km^2 to all of the estimates for consistency with the Mahoney *et al.* estimates. This implicitly assumed that the ice extent for this northern region of the Siberian Arctic remained complete over the 1901–1933 period.

Also, the Frolov *et al.* Siberian estimates nominally represented the mean sea ice extents for August, rather than for the entire July–September summer season. From Figure 2, we can see that the mean August sea ice extents are a reasonable proxy for the mean summer sea ice extents. Therefore, for this earlier period, we used the Frolov *et al.* "August" estimates as a proxy for Siberian summer sea ice extents. However, as we will discuss in Section 4, these estimates were then rescaled to match the observed temperature relationship in the satellite era for the region using the entire summer season. Therefore, the *rescaled* Frolov *et al.* estimates used in our final reconstruction are representative of the entire summer season.

3.5 Other sea ice datasets

Although the main dataset used for assessing Arctic sea ice trends since the 1970s was the satellite-derived gridded dataset described in Section 3.2, there is a similar, yet slightly longer dataset (1972–present) derived from biweekly to weekly sea ice charts compiled by the US National Ice Center (NIC) (National Ice Center 2006). The primary data sources used by the compilers of these charts were the satellite data (including the 1972–1977 NIMBUS-5 satellite mentioned in the introduction), and so the trends from both datasets are quite similar.

The most popular sea ice dataset used by the scientific community in recent years is the Hadley Centre's HadISST dataset (Rayner *et al.* 2003, Titchner and Rayner 2014). However, as mentioned in Section 3.2, for the pre-satellite era, the HadISST dataset is predominantly based on the Walsh dataset and so for our analysis we used the Walsh dataset directly instead. For version 1 of the HadISST, the post-1978 estimates are derived from the satellite estimates (Rayner *et al.* 2003). However, at the time of writing, version 2 of the HadISST dataset was in development, and for this version, the post-1972 period is derived from the NIC sea ice charts instead (Titchner and Rayner 2014).

Meier *et al.* (2012) have noted some inconsistencies between version 1 of the HadISST dataset and the satellite-based estimates during the satellite era. For this reason, they adjusted the 1953–1978 period of the HadISST dataset to create a more consistent 1953–2011 data series.

In this paper, we confine our analysis to the Arctic region. However, as mentioned in Section 2, there are also some useful datasets that provide information about seasonal sea ice trends in some of the non-Arctic seas in the Northern Hemisphere (e.g. Hill *et al.* 2002, Mahoney *et al.* 2011).

In Section 5, we compare our Arctic summer sea ice extent estimates to several alternative estimates of September Arctic sea ice extent trends:

- Pirón and Pasalodos (2016)
- Alekseev *et al.* (2016);
- Global Climate Model (GCM) hindcasts from the IPCC CMIP5 project.

The Pirón and Pasalodos (2016) estimates were taken from the supplementary information of their paper, downloaded from http://dx.doi.org/10.5281/zenodo.44756 *[Accessed 6th February 2016]*. The Alekseev *et al.* (2016) estimates were obtained from personal communication. The GCM hindcasts were digitized from Figure 3 of Overland and Wang (2013).

4 Regional Arctic analyses

Table 3 lists the linear relationships between seasonal surface air temperature anomalies (relative to 1961–1990) and seasonal sea ice extents for each of the three Arctic regions during the 1978–2015 satellite era, as determined using linear least squares fitting. In the Supplementary Information, the linear relationships are also plotted graphically, along with a brief review of the relevance of the statistics.

When we consider the slopes for each of the regions and seasons, we can see that the response of sea ice extent to temperature changes is quite pronounced for the Nordic Arctic for all seasons, but for the North American and Siberian Arctic it is mostly a summer phenomenon (and to a lesser extent an autumn phenomenon). For the Siberian winter and spring, the slopes of the lines are very small relative to the total sea ice extent, at only −100 km^2/°C and −600 km^2/°C, respectively. This is because the Siberian region is effectively ice packed during these seasons. This is also apparent from the fact that the r^2 values for these fits are negligible.

Table 4 describes the equivalent linear relationships between seasonal surface air temperatures and seasonal sea ice extents, according to the non-calibrated pre-satellite era datasets, during the pre-satellite era, 1901–1978 (or 1940s–1978 in the case of some of the Russian data-

Table 3. Linear least squares regression fits between seasonal sea ice extent (y, km^2) and temperature anomalies (x, °C) for the three Arctic regions during the satellite era, 1979–2015. Fits that are significant to >95% ($p < 0.05$) are in bold.

Season	Equation of line	r^2	p
North American Arctic			
Winter	$y = -28\,000x + 5\,788\,000$	0.28	**<0.001**
Spring	$y = -17\,000x + 5\,702\,000$	0.08	0.08
Summer	$y = -408\,000x + 3\,595\,000$	0.52	**<0.001**
Autumn	$y = -129\,000x + 5\,441\,000$	0.55	**<0.001**
Annual	$y = -123\,000x + 5\,153\,000$	0.58	**<0.001**
Nordic Arctic			
Winter	$y = -182\,000x + 2\,702\,000$	0.49	**<0.001**
Spring	$y = -302\,000x + 2\,591\,000$	0.62	**<0.001**
Summer	$y = -164\,000x + 1\,404\,000$	0.36	**<0.001**
Autumn	$y = -206\,000x + 2\,139\,000$	0.59	**<0.001**
Annual	$y = -247\,000x + 2\,233\,000$	0.64	**<0.001**
Siberian Arctic			
Winter	$y = -100x + 4\,459\,000$	0.00	0.77
Spring	$y = -600x + 4\,458\,000$	0.01	0.67
Summer	$y = -486\,000x + 3\,616\,000$	0.40	**<0.001**
Autumn	$y = -23\,000x + 4\,442\,000$	0.19	**0.005**
Annual	$y = -110\,000x + 4\,276\,000$	0.54	**<0.001**

sets). Unlike the satellite era results in Table 3, very few of the regions and seasons demonstrate a strong relationship between surface air temperatures and ice extents, and whenever they do, the relationships tend to be much weaker (e.g. smaller slopes and r^2 values).

This breakdown in the apparent temperature–sea ice relationship for the pre-satellite estimates has been noted by others (e.g. Semenov and Latif 2012, Parker and Ollier 2015). For instance, Semenov and Latif (2012) argued that the winter sea ice extent variability implied by the Walsh dataset is much less than would be expected from the observed temperature trends. Parker and Ollier (2015) also noted that the pre-1953 Walsh dataset does not seem to demonstrate the sea ice variability implied by Arctic temperature trends, although their claim that the Walsh dataset conflicts with the Danish Meteorological Institute's 1901–1956 sea ice charts is debatable since, as discussed in Section 3.3, Kelly's (1979) digitization of those sea ice charts was actually the primary data source for the pre-1953 Walsh dataset.

We argue that this apparent breakdown (or at least weakening) in the relationships between sea ice and temperature before the satellite era is *not* genuine, but rather a consequence of the poorer quality of the pre-satellite sea ice extent estimates. Indeed, the current climate models assume a strong relationship holds between sea ice and temperature (e.g. Kauker *et al.* 2008). Hence, we recalibrated the regional sea ice extent estimates so that they have a more consistent relationship to regional temperatures over the entire 1901–2015 period.

Figure 6 illustrates the seven-step procedure we used for our Arctic sea ice extent reconstructions for each season and region, using the North American Arctic summer as a case study. In the rest of this section, we provide a discussion of the data for each of our three Arctic regions (North American, Nordic and Siberian). In the Supplementary Information, we include additional

Table 4. Linear least squares regression fits between seasonal sea ice extent (y, km^2) and temperature anomalies (x, °C) for the three Arctic regions during the pre-satellite era before recalibration, 1901–1978. Fits that are significant to >95% ($p < 0.05$) are in bold.

Season	Equation of line	r^2	p
North American Arctic (Walsh dataset)			
Winter	$y = -4000x + 6\,192\,000$	0.03	0.15
Spring	$y = -9000x + 6\,146\,000$	0.02	0.25
Summer	$y = -117\,000x + 4\,246\,000$	0.06	**0.04**
Autumn	$y = -1000x + 6\,047\,000$	0.00	0.79
Annual	$y = -26\,000x + 5\,660\,000$	0.07	**0.02**
Nordic Arctic (Walsh dataset)			
Winter	$y = -57\,000x + 3\,001\,000$	0.19	**<0.001**
Spring	$y = -124\,000x + 2\,970\,000$	0.13	**0.001**
Summer	$y = -201\,000x + 1\,845\,000$	0.16	**<0.001**
Autumn	$y = -51\,000x + 2\,590\,000$	0.13	**<0.001**
Annual	$y = -122\,000x + 2\,605\,000$	0.24	**<0.001**
Siberian Arctic (Walsh dataset)			
Winter	$y = 4\,581\,000$, i.e. constant	N/A	N/A
Spring	$y = -200x + 4\,581\,000$	0.02	0.24
Summer	$y = -93\,000x + 4\,138\,000$	0.06	**0.04**
Autumn	$y = 4\,581\,000$, i.e. constant	N/A	N/A
Annual	$y = -7000x + 4\,470\,000$	0.01	0.41
Siberian Arctic (Russian datasets)			
Winter	$y = -11\,000x + 4\,152\,000$ (over 1940–1978 period)	0.04	0.22
Spring	$y = -29\,000x + 4\,073\,000$ (over 1940–1978 period)	0.15	**0.01**
Summer	$y = -97\,000x + 3\,455\,000$ (over 1900–1978 period)	0.05	**0.04**
Autumn	$y = +16\,000\,x + 3\,715\,000$ (over 1943–1978 period)	0.01	0.59
Annual	$y = -44\,000\,x + 3\,827\,000$ (over 1943–1978 period)	0.09	0.08

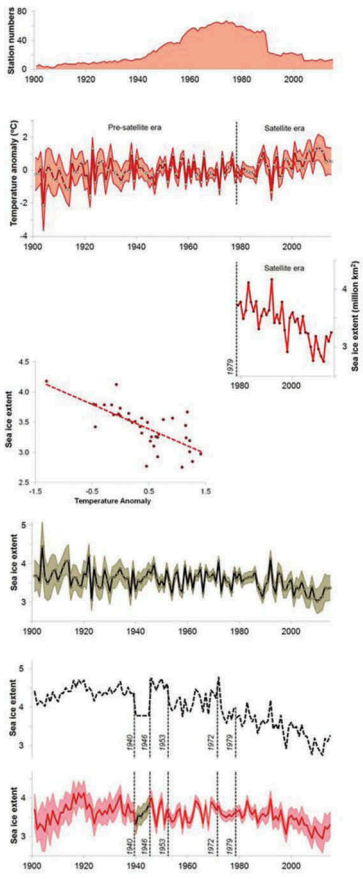

Step 1. Compile all available rural weather stations with temperature records for appropriate region (here, North American Arctic) and season (here, July to September, i.e., Summer).

Step 2. Construct gridded surface air temperature trends for that region and season. Error bars represent twice the standard error of the mean, i.e., the "confidence interval" (CI) and tend to be largest when the station numbers are lowest and/or when disagreement between stations is greatest.

Step 3. Calculate the mean sea ice extents for that season and region using satellite observations for the satellite era, i.e., 1979 – present.

Step 4. Calculate the best-fit linear relationship between mean surface air temperature trends and sea ice extent for that region and season over the satellite era, using linear least squares fitting of the datasets in steps 2 and 3.

Step 5. Apply the above linear relationship to the surface air temperature reconstruction from step 2 to generate a temperature-derived sea ice extent proxy for 1901 – present. This step is applied separately to the mean, upper bound and lower bound to generate equivalent confidence intervals for the proxy dataset.

Step 6. Calculate the mean sea ice extents estimated from the available pre-satellite dataset for that season and region. Group the estimates into separate periods according to the underlying data sources used. Note for our analysis, we use the satellite-derived estimates for the post-1979 satellite era.

Step 7. Separately rescale the estimates for each of the periods so that their means and standard deviations are the same as for the temperature-derived proxies. The confidence intervals of the temperature-derived proxies are used as an estimate of the associated uncertainty of the final reconstruction. For periods when the pre-satellite estimates are missing data (or are just climatology estimates), the temperature-derived proxies are used directly.

Figure 6. Schematic illustrating the seven-step procedure used to construct our seasonal sea ice extent reconstructions for each of our three Arctic regions, using North American Arctic summer as a case study.

statistical analysis of the residuals from the linear fits in Step 4, including an assessment of the corresponding Durbin–Watson statistics.

4.1 North American Arctic

For the pre-satellite era (1901–1978), we used the gridded Walsh dataset (version 1). However, as discussed in Section 3.3, the sources used for the Walsh dataset are different for different periods:

- 1901–1939: DMI sea ice charts for summer and spring; DMI ship reports for winter; fixed climatology for autumn
- 1940–1945: Fixed climatology since data were sparse during World War 2
- 1946–1952: As for 1901–1939, but with a greater and more consistent observation network
- 1953–1971: Sea ice charts from multiple sources (US Navy, British Meteorological Office, Canadian Meteorological Service, DMI)
- 1972–1978: NIC sea ice charts
- 1979–2015: Satellite data

In particular, the data available for the pre-1953 period are quite limited. Moreover, it can be seen from Figure 7 that for 1940–1945 (i.e. during World War 2), the Walsh dataset just provides a constant climatology and does not provide any estimates of trends during this period. The Walsh dataset does not contain much data for the pre-1952 autumn, so most of these autumn estimates are also just climatology values.

Following the procedure in Figure 6, in an attempt to correct for these changes in data sources, we separately rescaled the estimates from the Walsh dataset in each of the different periods (1901–1939, 1946–1952, 1953–1971 and 1972–1978) so that the means and standard deviations over each period were the same as the equivalent periods for our temperature-based sea ice extent proxy.

For the missing 1940–1945 period (and the longer missing period for autumn, i.e. 1901–1952), we replaced the constant Walsh climatology values with our temperature-based proxy estimates directly. For the satellite era (1979–2015), we used the more comprehensive estimates determined from the satellite data (Section 3.2). However, the standard deviations of the satellite dataset are larger than our temperature-based proxy for 1979–2015. Therefore, in order to maintain

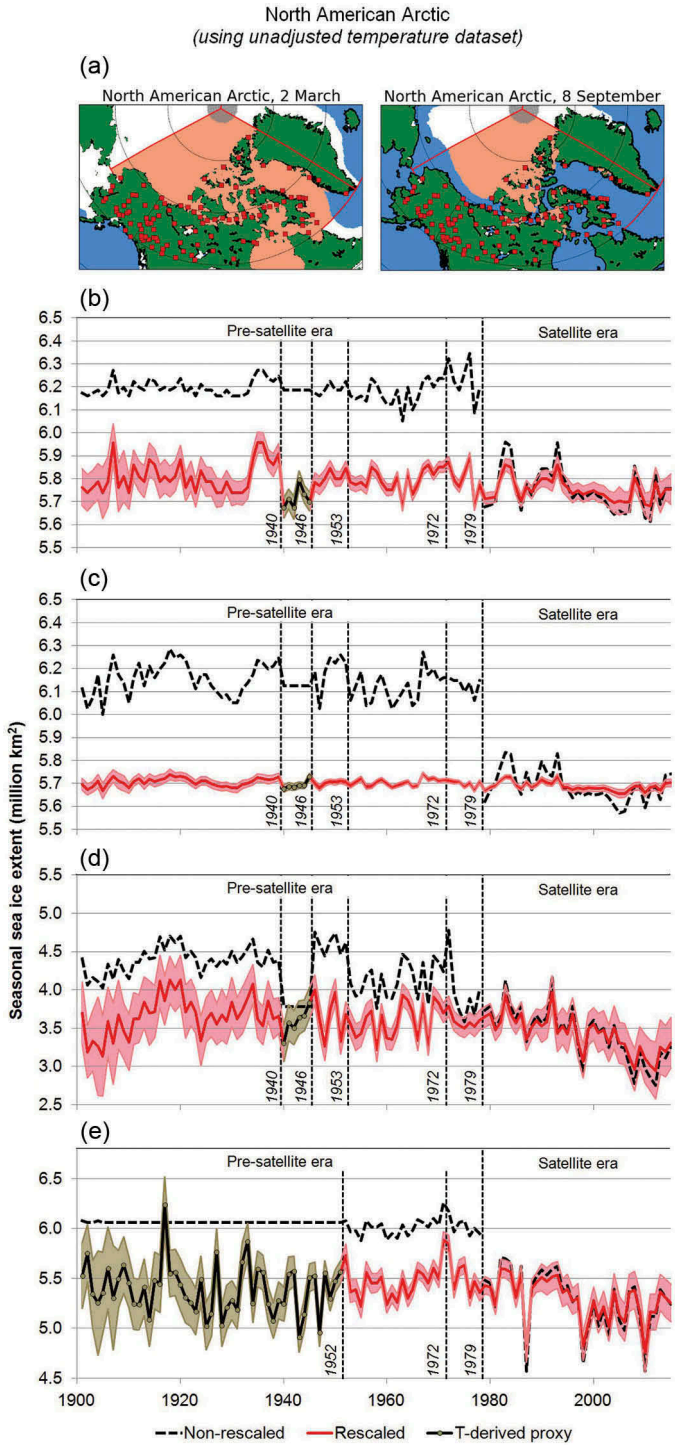

Figure 7. (a) The mean sea ice extents, and station locations for the North American Arctic region. (b)–(e) North American Arctic sea ice extent trends before and after rescaling for each season: (b) winter, (c) spring, (d) summer, (e) autumn. Note that the *y*-axes are different for each season.

consistency between the pre- and post-satellite eras, we also rescaled the satellite estimates to have the same means and standard deviations for this period.

The seasonal trends from the various estimates before and after rescaling are shown in Figure 7. As described in Figure 6, the uncertainty bands associated with our rescaled estimates are derived from the confidence intervals of the temperature-based sea ice proxies. A consequence of this is that the associated error bars for our rescaled regional datasets tend to be smallest when there are many weather stations and greatest when the number of weather stations is low. As can be seen from Figure 3(d), for the North American Arctic (and also the Nordic Arctic), the number of weather stations was greatest during the period

1951–1990. Hence, the associated error bars for our reconstruction are larger both before 1951 and after 1990.

4.2 Nordic Arctic

The data sources and procedure for rescaling the Nordic Arctic estimates were basically the same as for the North American Arctic, and we therefore limit the discussion of this region to avoid repetition. The seasonal trends from the various estimates before and after rescaling are shown in Figure 8. The main differences between the Nordic and North American Arctic reconstructions are:

- There is considerable variability in Nordic Arctic sea ice extents for all four seasons, while for the North American Arctic variability is much greater for the summer and much lower for the spring.
- For the pre-satellite era, the Walsh dataset generally had more observations for the Nordic Arctic than for the North American Arctic.

As for the North American Arctic region, for the pre-1953 portion of the Walsh dataset, the autumn values are essentially just climatology values. Therefore, as discussed in Figure 6, we replaced this period directly with our temperature-based proxy. However, for the winter values, although the Walsh dataset nominally implies some variability, it can be seen from Figure 8(b) that there is almost no variability in the dataset pre-1953 compared with the post-1953 period. This suggests that the Walsh dataset estimates for the pre-1953 winter values are also little more than climatology estimates. Therefore, it could be argued that it might be more realistic to treat them in the same way as the autumn estimates. However, since the Walsh dataset included *some* slight variability, we cautiously treated this period of their estimates as non-climatology (except for the 1940–1945 period).

4.3 Siberian Arctic

As discussed in Section 3.4, the version of the Walsh dataset we used contained almost no observations for the Siberian Arctic region before the satellite era. On the other hand, the Russian-based AARI group have compiled several datasets of pre-satellite era observations for the Siberian Arctic (Zakharov 1997, Polyakov *et al.* 2003, Arctic and Antarctic Research Institute (AARI) 2007, Mahoney 2008, Mahoney *et al.* 2008, Frolov *et al.* 2009). Hence, for the Siberian Arctic region, we used the Russian sea ice datasets for the pre-satellite era instead of the Walsh dataset. Below are the different sources for the Siberian Arctic reconstruction:

- 1901–1932: No estimates for most seasons, but Frolov *et al.* (2009) have developed a rough estimate of August trends using a variety of sources including descriptions of early Arctic voyages and other observations. We used this as a proxy for summer trends.
- 1933–1952: Systematic aircraft reconnaissance 1–3 times per month with some additional ship and coastal observations
- 1953–1971: As for 1933–1952, but with improved frequency and coverage, as well as additional observations from a network of drifting buoys and, beginning in the late 1960s, some early satellite observations
- 1972–1978: As for 1953–1971, but with improved satellite technology
- 1979–2015: NSIDC satellite data

The seasonal trends from the various estimates before and after rescaling are shown in Figure 9. We also show the equivalent non-rescaled estimates from the original Walsh dataset. Although there is *some* variability in Siberian Arctic summer sea ice extent implied by the Walsh dataset for the pre-satellite era, it is very inconsistent and modest compared with the satellite-era estimates. Apparently the latest version of the Walsh dataset will incorporate the AARI datasets (Walsh *et al.* 2015, 2017). So, this particular limitation of the earlier Walsh datasets (and related datasets such as HadISST) should no longer be a problem for analysis based on the newer version.

Interestingly, the AARI datasets actually imply that there was quite a bit of variability in the winter, spring and autumn seasons for the pre-satellite era. However, as discussed earlier, satellite observations suggest that the Siberian Arctic remains mostly ice packed for the winter and spring, and that autumn variability is quite modest. Therefore, unlike in the other two regions, our rescaling for these seasons considerably reduces the implied variability for the pre-satellite era. Finally, it is worth noting from Figure 3(d) that the number of Siberian Arctic weather stations in our temperature dataset dropped rather dramatically after 1990. As a result, there is some increase in the uncertainty of our Siberian summer reconstructions after 1990, since our confidence intervals are derived from our temperature-based proxies.

5 Arctic sea ice extent trends (1901–2015)

Figure 10 sums the seasonal reconstructions from the three Arctic regions described in the previous section to yield seasonal reconstructions for the entire Arctic region. Figure 10(e) plots the annual reconstruction, which is simply the average of the four seasons. The plots labelled "non-rescaled" correspond to the equivalent estimates calculated from the Walsh

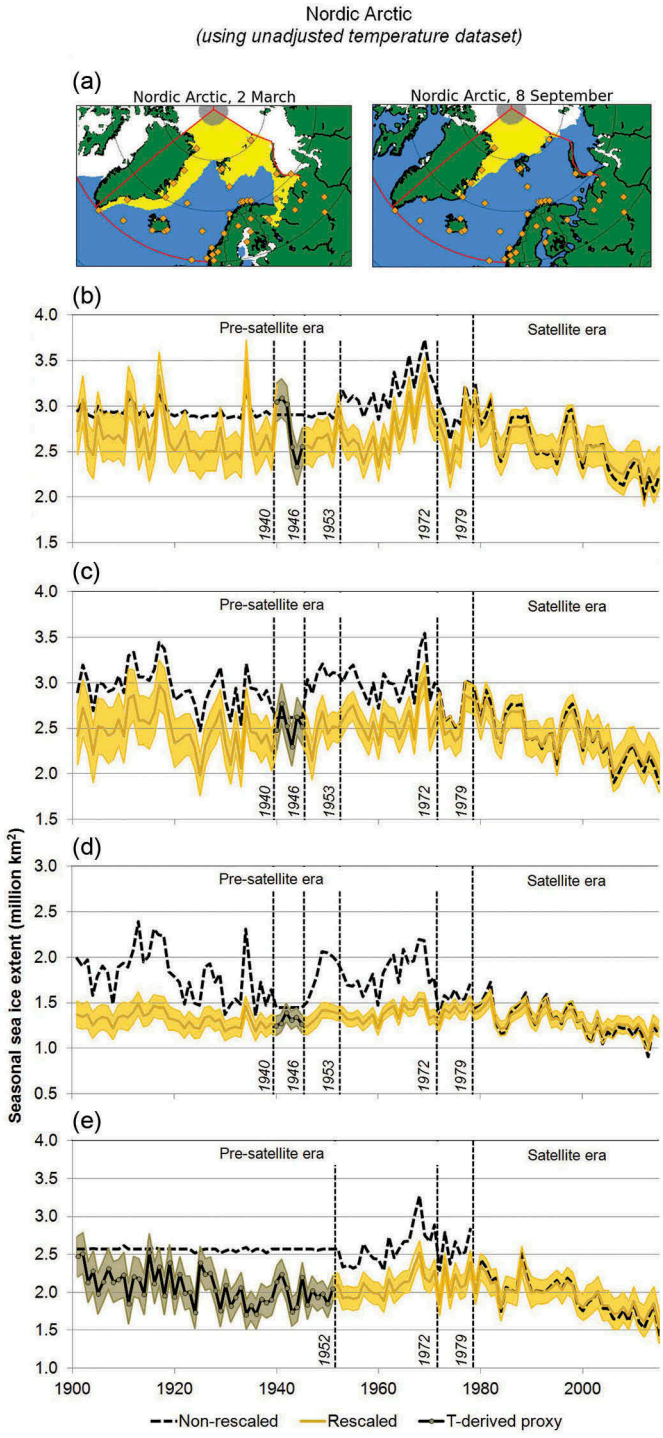

Figure 8. (a) The mean sea ice extents, and station locations for the Nordic Arctic region. (b)–(e) Nordic Arctic sea ice extent trends before and after rescaling for each season: (b) winter, (c) spring, (d) summer, (e) autumn. Note that the *y*-axes are different for each season.

dataset for the pre-satellite era and NSIDC data for the satellite era.

For all seasons and the annual average, we can see that the average sea ice extent has been generally decreasing since the late 1970s, which agrees with the analysis of those studies that considered only the satellite era (e.g. Comiso *et al.* 2008, Cavalieri and Parkinson 2012, Meier *et al.* 2014). However, it appears that the late 1970s coincided with a reversal in trends. From the mid 1940s until the late 1970s, the average sea ice extent was instead generally increasing. Before the 1940s, the trends are less clear; for example, while summer extents seem to have been generally increasing from the start of the century until the 1940s, the

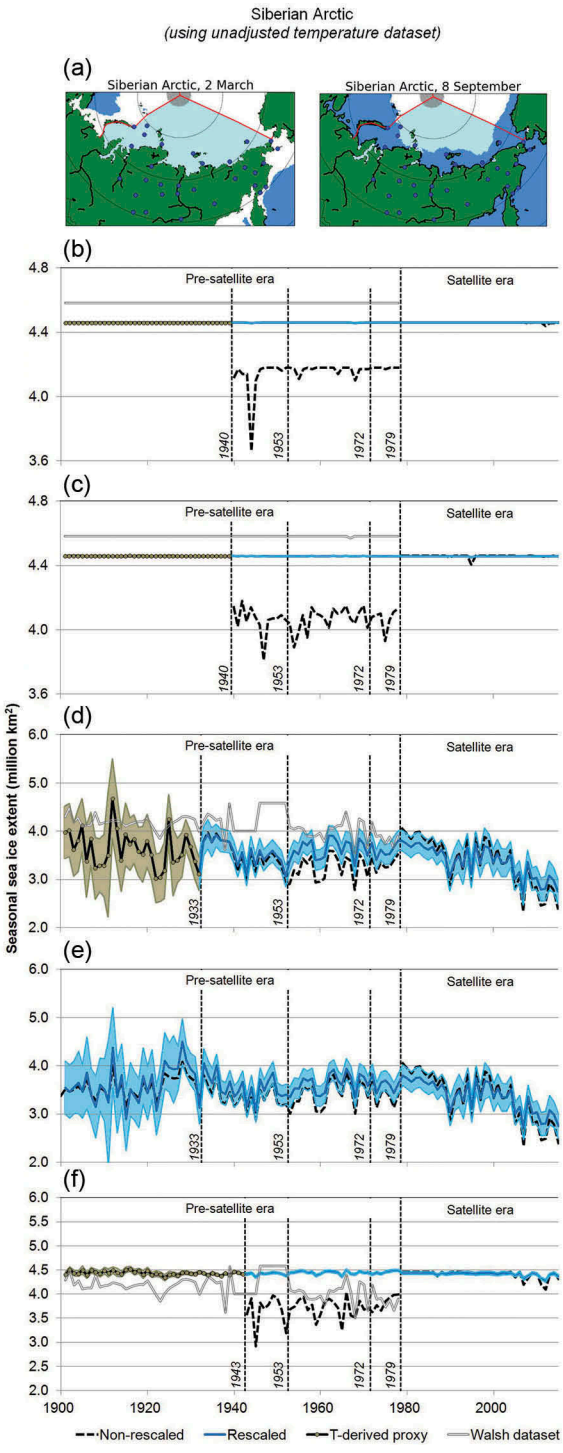

Figure 9. (a) The mean sea ice extents, and station locations for the Siberian Arctic region. (b)–(f) Siberian Arctic sea ice extent trends before and after rescaling for each season. Two different rescaled estimates for summer trends are provided: (d) and (e). (b) Winter, (c) spring, (d) summer using Mahoney (2008) dataset; (e) summer using Frolov *et al.* (2009) dataset; (f) autumn. Note that the *y*-axes are different for each season.

opposite seems to have been occurring for autumn extents. Nonetheless, it is clear that the general decline in Arctic sea ice extent during the satellite era is less dramatic when considered in the context of the entire 1901–2015 record.

A lot of the discussion of Arctic sea ice trends has focused on the summer trends, in particular those during the month of September (i.e. the peak of Arctic summer). In Figure 11, we compare our summer Arctic reconstruction (Fig. 11(e)) with several other reconstructions (Fig. 11(a)–(d)) that have been discussed in the literature.

Figure 11(a) shows the equivalent estimate from the Walsh dataset. Although our reconstruction agrees that the average Arctic summer sea ice extents have been decreasing since the late 1970s, the non-rescaled Walsh dataset estimates suggest that sea ice extents were fairly constant during the pre-satellite era, fluctuating about a mean summer sea ice extent of ~10 million km^2. However, our reconstruction implies much more variability during the pre-satellite era. In particular, the post 1970s decrease seems to have followed a period of generally increasing extents since the mid 1940s.

Figure 11(b) and (c) show the September reconstructions of Pirón and Pasalodos (2016) and Alekseev *et al.* (2016), respectively. As we saw from Figure 2, mid September marks the peak of the Arctic summer and so we would expect September sea ice extents to be generally lower than the summer averages, and the Pirón and Pasalodos (2016) reconstruction consistently is so. The Alekseev *et al.* (2016) reconstruction was provided to us (personal communication) as a relative anomaly index instead of absolute values. Therefore, for comparison with our reconstruction, we added a value of 6.37 million km^2 to all of the anomaly indices so that the mean September ice extent for the Pirón and Pasalodos (2016) and Alekseev *et al.* (2016) reconstructions were the same over the 1980–2013 period.

As the Pirón and Pasalodos (2016) and Alekseev *et al.* (2016) reconstructions are monthly averages while our reconstruction is a seasonal average, we might expect that our summer reconstruction would show less variability than the two September reconstructions. Nonetheless, the long-term trends of these two reconstructions seem closer to our summer reconstruction than to the Walsh summer reconstruction; for example, they both indicate Arctic sea ice growth from the 1940s up to the late 1970s.

Like our reconstruction, the Pirón and Pasalodos (2016) used the Russian sea ice datasets (Section 3.4) for the Siberian Arctic region, while the original Walsh dataset did not. This could explain the better fit to our reconstruction. Meanwhile, the Alekseev *et al.* (2016) reconstruction was a temperature-based proxy for sea ice extents. As described in Figure 6, we used similar

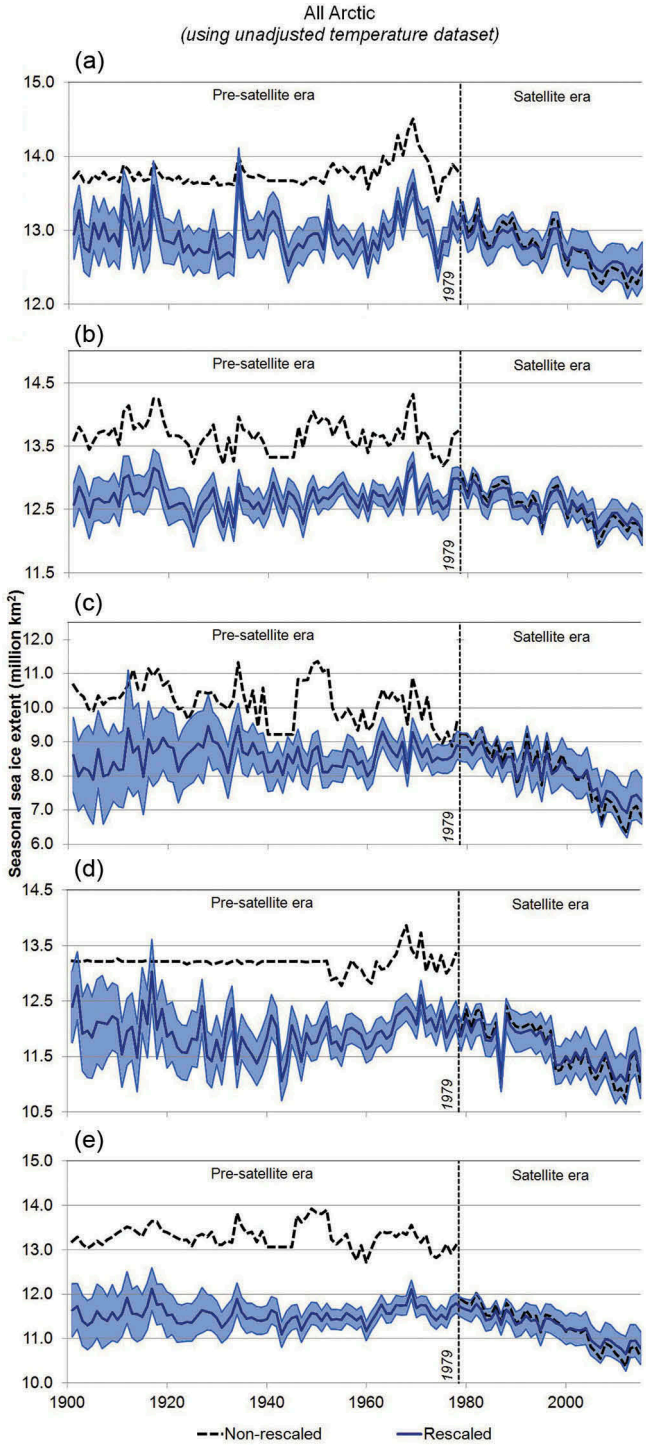

Figure 10. All-Arctic seasonal and annual trends: (a) winter, (b) spring, (c) summer, (d) autumn, (e) annual.

temperature-based proxies for recalibrating our data sources. So, it is perhaps not too surprising that they should imply similar trends.

However, there are some notable differences between our summer reconstruction and the Pirón and Pasalodos (2016) and Alekseev *et al.* (2016) September reconstructions. While the trends of our summer reconstruction and the Pirón and Pasalodos (2016) September reconstruction seem to track each other quite well from the start of the Pirón and Pasalodos reconstruction in 1935 until the 1990s, after this time, the Pirón and Pasalodos reconstruction suggests a more dramatic decline in sea ice extent. As a result, according to the Pirón and Pasalodos reconstruction, the low sea ice extents since the late 1990s appear unprecedented (at least

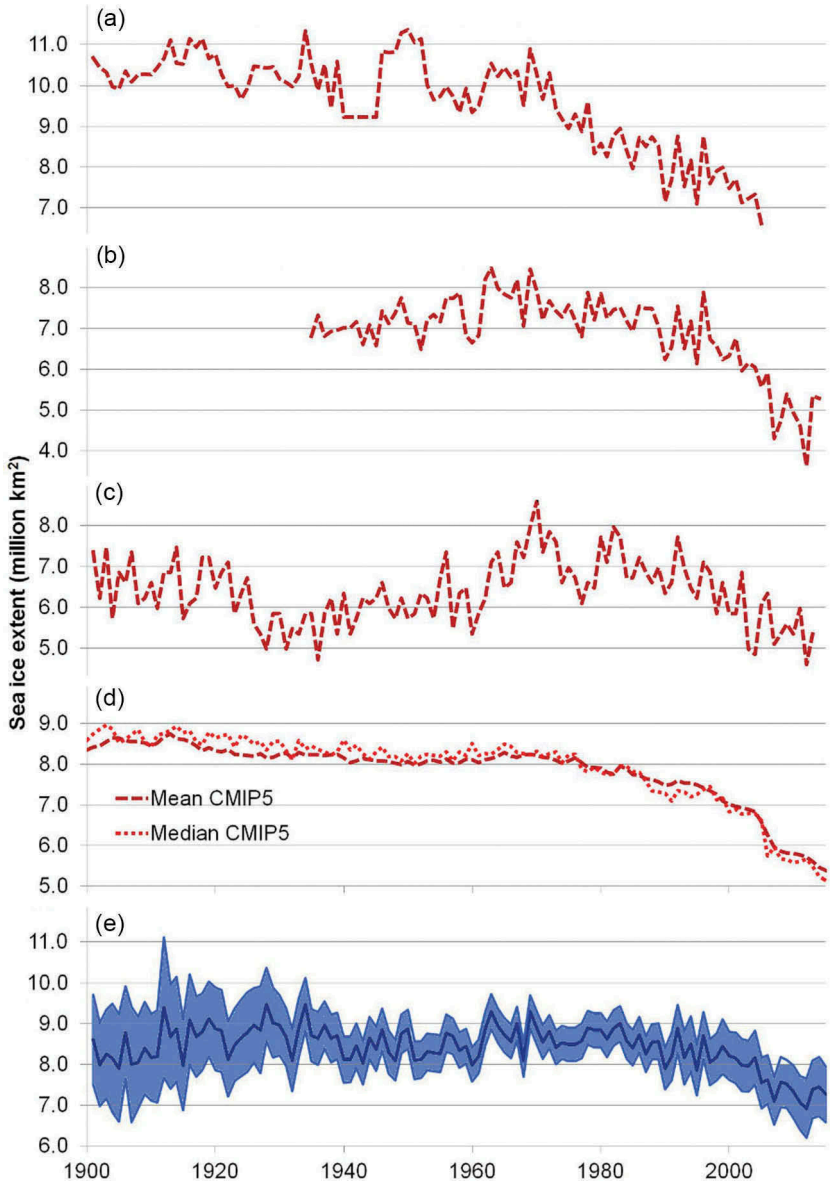

Figure 11. Comparison of our all-Arctic summer sea ice extent reconstruction with several other estimates in the literature: (a) Walsh dataset-derived summer extents; (b) Pirón and Pasalodos (2016) September extents; (c) Alekseev *et al.* (2016) September extents; (d) CMIP5 modelled September extents; (e) our summer reconstruction.

over the period considered by the reconstruction). On the other hand, the Alekseev *et al.* (2016) reconstruction implies a greater decline in sea ice extent during the early 20th century *and* a greater increase in sea ice extent from the 1940s until the 1970s than our reconstruction. As a result, according to the Alekseev *et al.* (2016) reconstruction, the relatively low sea ice extents of the last decade or so were actually comparable to those in the 1930s.

We will consider this contentious issue of how recent Arctic sea ice extents compare to those during the pre-satellite era in more detail below. However, in Figure 11(d), we plot the September Arctic sea ice extent "hindcasts"[3] of the Coupled Model Intercomparison Project Phase 5 (CMIP5) climate models, which are the climate models used for the most recent Intergovernmental Panel on Climate Change (IPCC) reports.

Figure 11(d) plots both the mean and median hindcasts from 36 CMIP5 models (with an average of ~2.5 ensemble members per model) which were obtained by digitizing Figure 3 of Overland and Wang (2013). We use these two plots to represent the trends of the

[3]A "hindcast" is like a forecast except that it is a retrospective "prediction" of what should have occurred in the past, rather than what is expected to occur in the future.

CMIP5 hindcasts rather than (for instance) the upper and lower envelopes of the CMIP5 hindcasts because there is a remarkable inconsistency between CMIP5 models in the modelled September Arctic sea ice extent. That is, the average 20th century extents predicted by each of the models varied from an unrealistically low ~4 million km^2 to unrealistically high ~12 million km^2; see Figure 3 of Overland and Wang (2013) or the comparable Figure 2 of Stroeve *et al.* (2012). As a result, the collective envelope of the entire ensemble of CMIP5 models covers such an unrealistically large range of "average extents" that it would nominally "contain" almost any physically plausible scenario for sea ice extent trends since 1901. In other words, the collective envelope is effectively too wide to provide much scientific information other than the fact that the CMIP5 models have considerable difficulty in reproducing the expected September Arctic sea ice extent.

Despite that, the fact that the mean and median CMIP5 hindcasts are so similar to each other indicates that the hindcasted *trends* in sea ice extents (as opposed to absolute values) are remarkably similar for all 36 models. With this in mind, it is striking that they fail to capture almost any of the variability over the pre-satellite era shown by our summer reconstruction. Specifically, the CMIP5 hindcasts imply that September Arctic sea ice extent remained fairly constant for most of the 20th century up until the late 1970s/early 1980s, after which the September extent began to decrease at an accelerating rate.

Figure 12 shows an expanded version of our annual all-Arctic sea ice extent reconstruction, i.e. the main plot from Figure 10(e). If we temporarily exclude the confidence intervals and focus on the reconstruction means (thick central line), then it seems that up until 2005, the lowest average Arctic sea ice extent was in 1943, but that every year since 2004 has been lower than that 1943 minimum (red dashed line). Indeed, Overland *et al.* (2012, 2015) have suggested that recent years may have seen a persistent shift in Arctic atmospheric circulation which could be consistent with a shift to relatively low Arctic sea ice extents.

However, if we also consider the full envelope of the associated confidence intervals, we cannot rule out the possibility that similarly low sea ice extents occurred during the 20th century. That is, the upper bounds of the estimates for all years since 2004 are still greater than the lower bounds for several years in the early 20th century.

6 Conclusions

In this article, we developed and presented a new dataset describing seasonal and annual Arctic sea ice extents for the period 1901–2015. Our dataset consists of separate seasonal indices for three Arctic regions (North American, Nordic and Siberian) as well as composite indices for the entire Arctic Ocean and seas, although excluding those non-Arctic Northern Hemisphere seas with seasonal sea ice (e.g. Sea of Okhotsk, Bering Sea, Gulf of St Lawrence).

According to this new dataset, the recent period of Arctic sea ice retreat since the 1970s followed a period of sea ice growth after the mid 1940s, which in turn followed a period of sea ice retreat after the 1910s. Our reconstructions agree with previous studies that have noted a general decrease in Arctic sea ice extent (for all four seasons) since the start of the satellite era (1979). However, the timing of the start of the satellite era is unfortunate in that it coincided with the end of several decades during which Arctic sea ice extent was generally increasing.

This late-1970s reversal in sea ice trends was *not* captured by the hindcasts of the recent CMIP5 climate models used for the latest IPCC reports, which suggests

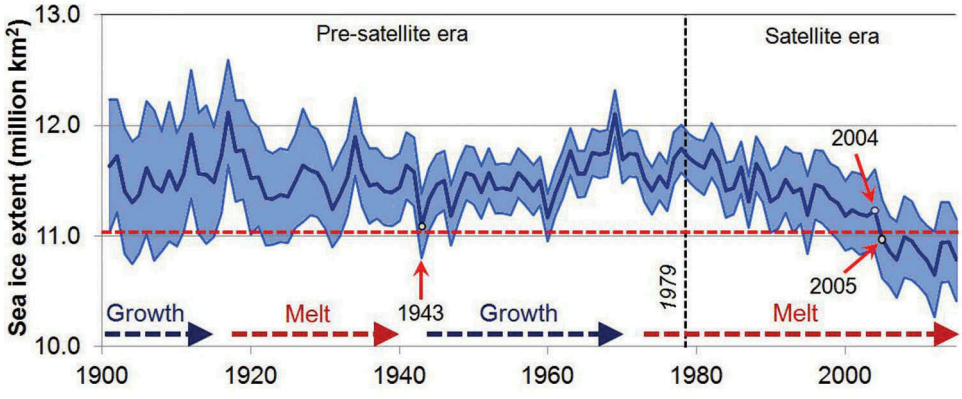

Figure 12. Comparison of annual Arctic sea ice extent trends during the pre-satellite era with the satellite era. Periods of general sea ice growth and periods of general sea ice melt are indicated at the bottom of the figure.

that current climate models are still quite poor at modelling past sea ice trends. Nor is it described in previous Arctic sea ice reconstructions such as the Walsh dataset or the widely used HadISST sea ice dataset, although some recent studies have noted similar reversals, e.g. Pirón and Pasalodos (2016) and Alekseev *et al.* (2016).

As we saw from Figure 1, and Tables 1 and 2, Arctic sea ice is a key component of the Arctic hydrological cycle. So, this new dataset should be of use for improving our understanding of Arctic hydrology.

Acknowledgements

We thank Professor Genrikh Alekseev of the Arctic and Antarctic Research Institute for providing the Alekseev *et al.* (2016) September sea ice extent estimates used in Figure 11. We would also like to thank the editor and reviewers for their constructive comments.

All of the research in this collaborative paper was carried out during the authors' free time and at their own expense. None of the authors received any funding for this research. The underlying research materials for this article can be accessed at https://doi.org/10.6084/m9.figshare.4879565.v3.

Disclosure statement

No potential conflict of interest was reported by the authors.

ORCID

Ronan Connolly http://orcid.org/0000-0001-5843-3544

References

Aagaard, K. and Carmack, E.C., 1989. The role of sea ice and other fresh water in the Arctic circulation. *Journal of Geophysical Research*, 94C, 14485–14498. doi:10.1029/JC094iC10p14485

ACSYS, 2003. ACSYS historical ice chart archive (1553-2002). IACPO Informal Report No. 8. Tromsø, Norway: Arctic Climate System Study. Available from: http://www.climate-cryosphere.org/resources/historical-ice-chart-archive [Accessed 16 January 2016].

Alekseev, G., Glok, N., and Smirnov, A., 2016. On assessment of the relationship between changes of sea ice extent and climate in the Arctic. *International Journal of Climatology*, 36, 3407–3412. doi:10.1002/joc.4550

Arctic and Antarctic Research Institute (AARI), 2007. *Sea ice charts of the Russian Arctic in gridded format, 1933-2006*. Edited and compiled by V. Smolyanitsky et al. Boulder, CO: National Snow and Ice Data Center. doi:10.7265/N5D21VHJ

Bekryaev, R.V., Polyakov, I.V., and Alexeev, V.A., 2010. Role of polar amplification in long-term surface air temperature variations and modern Arctic warming. *Journal of Climate*, 23, 3888–3906. doi:10.1175/2010JCLI3297.1

Bengtsson, L., Semenov, V.A., and Johannessen, O.M., 2004. The early twentieth-century warming in the Arctic – A possible mechanism. *Journal of Climate*, 17, 4045–4057. doi:10.1175/1520-0442(2004)017<4045:TETWIT>2.0.CO;2

Bintanja, R. and Selten, F.M., 2014. Future increases in Arctic precipitation linked to local evaporation and sea-ice retreat. *Nature*, 509, 479–482. doi:10.1038/nature13259

Brönnimann, S., 2009. Early twentieth-century Arctic warming. *Nature Geoscience*, 2, 735–736. doi:10.1038/ngeo670

Brönniman, S., *et al.*, 2008. Can we reconstruct Arctic sea ice back to 1900 with a hybrid approach? *Climate of the past Discussions*, 4, 955–979. doi:10.5194/cpd-4-955-2008

Brönnimann, S., *et al.*, 2012. A multi-data set comparison of the vertical structure of temperature variability and change over the Arctic during the past 100 years. *Climate Dynamics*, 39, 1577–1598. doi:10.1007/s00382-012-1291-6

Cavalieri, D., *et al.*, 1996 (updated yearly). *Sea ice concentrations from Nimbus-7 SMMR and DMSP SSM/I-SSMIS passive microwave data, version 1*. Boulder, CO: National Snow and Ice Data Center. doi:10.5067/8GQ8LZQVL0VL

Cavalieri, D.J., Gloersen, P., and Campbell, W.J., 1984. Determination of sea ice parameters with the NIMBUS 7 SMMR. *Journal of Geophysical Research*, 89 (D), 5355–5369. doi:10.1029/JD089iD04p05355

Cavalieri, D.J. and Parkinson, C.L., 2012. Arctic sea ice variability and trends, 1979-2010. *The Cryosphere*, 6, 881–889. doi:10.5194/tc-6-881-2012

Cohen, J., *et al.*, 2014. Recent Arctic amplification and extreme mid-latitude weather. *Nature Geoscience*, 7, 627–637. doi:10.1038/ngeo2234

Comiso, J.C., *et al.*, 2008. Accelerated decline in the Arctic sea ice cover. *Geophysical Research Letters*, 35, L01703. doi:10.1029/2007GL031972

Curry, J.A., Schramm, J.L., and Ebert, E.E., 1995. Sea ice-albedo climate feedback mechanism. *Journal of Climate*, 8, 240–247. doi:10.1175/1520-0442(1995)008<0240:SIACFM>2.0.CO;2

Danish Meteorological Institute (DMI), and NSIDC, 2012. *Arctic sea ice charts from the Danish Meteorological Institute, 1893-1956*. Compiled by V. Underhill and F. Fetterer. Boulder, CO: National Snow and Ice Data Center. doi:10.7265/N56D5QXC

Day, J.J., *et al.*, 2012. *Environmental Research Letters*. 7, 034011. doi:10.1088/1748-9326/7/3/034011

Deser, C., *et al.*, 2010. The seasonal atmospheric response to projected Arctic sea ice loss in the late twenty-first century. *Journal of Climate*, 23, 333–351. doi:10.1175/2009JCLI3053.1

Dickson, R., *et al.*, 2007. Current estimates of freshwater flux through Arctic and subarctic seas. *Progress in Oceanography*, 73, 210–230. doi:10.1016/j.pocean.2006.12.003

Divine, D.V. and Dick, C., 2006. Historical variability of sea ice edge position in the Nordic Seas. *Journal of Geophysical Research*, 111, C01001. doi:10.1029/2004JC002851

Francis, J.A., *et al.*, 2009. Winter Northern Hemisphere weather patterns remember summer Arctic sea-ice extent. *Geophysical Research Letters*, 36, L07503. doi:10.1029/2009GL037274

Frolov, I.E., *et al.*, 2009. *Climate change in Eurasian Arctic shelf seas*. Berlin, Heidelberg: Springer Praxis Books. ISBN: 978-3-540-85874-4. doi:10.1007/978-3-540-85875-1

Guo, D., *et al.*, 2014. Mechanism on how the spring Arctic sea ice impacts the East Asian summer monsoon. *Theoretical and Applied Climatology*, 115, 107–119. doi:10.1007/s00704-013-0872-6

Haine, T.W.N., *et al.*, 2015. Arctic freshwater export: status, mechanisms, and prospects. *Global and Planetary Change*, 125, 13–35. doi:10.1016/j.gloplacha.2014.11.013

Hanna, E., *et al.*, 2012. Recent warming in Greenland in a long-term instrumental (1881-2012) climatic context: I. Evaluation of surface air temperature records. *Environmental Research Letters*, 7, 045404. doi:10.1088/1748-9326/7/4/045404

Hill, B., Ruffman, A., and Drinkwater, K., 2002. Historical record of the incidence of sea ice on the Scotian shelf and the Gulf of St. Lawrence. *Proceedings of the 16th IAHR International Symposium on Ice*, 2–6 December 2002 Dunedin, New Zealand. Available from: http://nparc.cisti-icist.nrc-cnrc.gc.ca/npsi/ctrl?action=shwart&index=an&req=8895102&lang=en [Accessed 17 February 2016].

Hinkel, K.M. and Nelson, F.E., 2007. Anthropogenic heat island at Barrow, Alaska during winter: 2001-2005. *Journal of Geophysical Research*, 112, D06118. doi:10.1029/2006JD007837

Holland, M.M., Finnis, J., and Serreze, M.C., 2006. Simulated Arctic Ocean freshwater budgets in the twentieth and twenty-first centuries. *Journal of Climate*, 19, 6221–6242. doi:10.1175/JCLI3967.1

Holland, M.M., *et al.*, 2007. Projected changes in Arctic Ocean freshwater budgets. *Journal of Geophysical Research*, 112, G04S55. doi:10.1029/2006JG000354

International Hydrographic Organization, 2002. Names and limits of oceans and seas. Special Publication No. 23, Draft 4th Ed., June 2002. Monaco: International Hydrographic Bureau. Available from: https://www.iho.int/mtg_docs/com_wg/S-23WG/S-23WG_Misc/Draft_2002/Draft_2002.htm http://epic.awi.de/29772/ [Accessed 28 January 2016].

Ivanova, N., *et al.*, 2015. Inter-comparison and evaluation of sea ice algorithms: towards further identification of challenges and optimal approach using passive microwave observations. *The Cryosphere*, 9, 1797–1817. doi:10.5194/tc-9-1797-2015

Johannessen, O.M., *et al.*, 2004. Arctic climate change: observed and modelled temperature and sea-ice variability. *Tellus A*, 56, 328–341. doi:10.1111/j.1600-0870.2004.00060.x

Kauker, F., *et al.*, 2008. Modeling the 20th century Arctic ocean/sea ice system: reconstruction of surface forcing. *Journal of Geophysical Research*, 446, C09027. doi:10.1029/2006JC004023

Kelly, P.M., 1979. An Arctic sea ice data set, 1901-1956. *Workshop on Snow Cover and Sea Ice Data. Worlds Data Center A for Glaciology. Report GD-5*. Available from: http://nsidc.org/data/docs/noaa/g02203-dmi/docs/Kelly_GD5_1979.pdf [Accessed 12 January 2016].

Konstantinov, P.I., Grishchenko, M.Y., and Varentsov, M.I., 2015. Mapping Urban Heat Islands of Arctic cities using combined data on field measurements and satellite images based on the example of the city of Apatity (Murmansk Oblast). *Izvestiya, Atmospheric and Oceanic Physics*, 61, 992–998. doi:10.1134/S000143381509011X

Kopec, B.G., *et al.*, 2016. Influence of sea ice on Arctic precipitation. *Proceedings of the National Academy of Science*, 113, 46–51. doi:10.1073/pnas.1504633113

Kuzmina, S.I., *et al.*, 2008. High northern latitude surface air temperature: comparison of existing data and creation of a new gridded data set 1900-2000. *Tellus*, 60A, 289–304. doi:10.1111/j.1600-0870.2008.00303.x

Kwok, R., Cunningham, G.F., and Pang, S.S., 2004. Fram Strait sea ice outflow. *Journal of Geophysical Research*, 109, C01009. doi:10.1029/2003JC001785

Landsea, C.W., *et al.*, 2008. A reanalysis of the 1911-20 Atlantic hurricane database. *Journal of Climate*, 21, 2138–2168. doi:10.1175/2007JCLI1119.1

Lawrimore, J.H., *et al.*, 2011. An overview of the global historical climatology network monthly mean temperature data set, version 3. *Journal of Geophysical Research*, 116, D19121. doi:10.1029/2011JD016187

Liu, J., *et al.*, 2012. Impact of declining Arctic sea ice on winter snowfall. *Proceedings of the National Academy of Sciences of the United States of America*, 109, 4074–4079. doi:10.1073/pnas.1114910109

Mahoney, A., 2008. *Sea ice edge location and extent in the Russian Arctic, 1933-2006*. Boulder, CO: National Snow and Ice Data Center. doi:10.7265/NSW37T8Z

Mahoney, A.R., *et al.*, 2008. Observed sea ice extent in the Russian Arctic, 1933-2006. *Journal of Geophysical Research*, 113, C11005. doi:10.1029/2008JC004830

Mahoney, A.R., *et al.*, 2011. Sea-ice distribution in the Bering and Chukchi Seas: information from historical whaleships' logbooks and journals. *Arctic*, 64, 465–477. doi:10.14430/arctic4146

Maslanik, J. and Stroeve, J., 1999 (updated daily). *Near real-time DMSP SSMIS daily polar gridded sea ice concentrations*. Boulder, CO: National Snow and Ice Data Center. doi:10.5067/8GQ8LZQVL0VL

Meier, W.N., *et al.*, 2012. A simple approach to providing a more consistent Arctic sea ice extent time series from the 1950s to present. *The Cryosphere*, 6, 1359–1368. doi:10.5194/tc-6-1359-2012

Meier, W.N., *et al.*, 2014. Arctic sea ice in transformation: a review of recent observed changes and impacts on biology and human activity. *Reviews of Geophysics*, 52, 185–217. doi:10.1002/2013RG000431

Menne, M.J. and Williams, C.N., 2009. Homogenization of temperature series via pairwise comparisons. *Journal of Climate*, 22, 1700–1717. doi:10.1175/2008JCLI2263.1

Miles, M.W., *et al.*, 2014. A signal of persistent Atlantic multidecadal variability in Arctic sea ice. *Geophysical Research Letters*, 41, 436–469. doi:10.1002/2013GL058084

Münchow, A., 2016. Volume and freshwater flux observations from Nares Strait to the west of Greenland at daily time scales from 2003 to 2009. *Journal of Physical Oceanography*, 46, 141–157. doi:10.1175/JPO-D-15-0093.1

National Ice Center, 2006 (updated 2009). *National Ice Center Arctic sea ice charts and climatologies in gridded format*. Edited and compiled by F. Fetterer and C. Fowler. Boulder, CO:National Snow and Ice Data Center. doi:10.7265/N5X34VDB

Overland, J., *et al.*, 2012. The recent shift in early summer Arctic atmospheric circulation. *Geophysical Research Letters*, 39, L19804. doi:10.1029/2012GL053268

Overland, J., *et al.*, 2015. The melting Arctic and midlatitude weather patterns: are they connected? *Journal of Climate*, 28, 7917–7932. doi:10.1175/JCLI-D-14-00822.1

Overland, J.E. and Wang, M., 2013. When will the summer Arctic be nearly sea ice free? *Geophysical Research Letters*, 40, 2097–2101. doi:10.1002/grl.50316

Parker, A. and Ollier, C.D., 2015. Is there a quasi-60 years' oscillation of the Arctic sea ice extent? *Journal of Geography, Environment and Earth Science International*, 2, 77–94. doi:10.9734/JGEESI/2015/16694

Parkinson, C.L. and Cavalieri, D.J., 1989. Arctic sea ice 1973-1987: seasonal, regional, and interannual variability. *Journal of Geophysical Research*, 94 (C10), 14499–14523. doi:10.1029/JC094iC10p14499

Perovich, D.K. and Polashenski, C., 2012. Albedo evolution of seasonal Arctic sea ice. *Geophysical Research Letters*, 39, L08501. doi:10.1029/2012GL051432

Peterson, B.J., *et al*., 2006. Trajectory shifts in the Arctic and subarctic freshwater cycle. *Science*, 313, 1061–1066. doi:10.1126/science.1122593

Pirón, M.Á.C. and Pasalodos, J.A.C., 2016. Nueva serie de extension del hielo marino ártico en septiembre entre 1935 y 2014. *Revista de Climatología*, 16, 1–19. (in Spanish). Available from: http://webs.ono.com/reclim/ [Accessed 6 February 2016].

Polyakov, I., *et al*., 2003. Long term variability in Arctic marginal seas. *Journal of Climate*, 16, 2078–2085. doi:10.1175/1520-0442(2003)016<2078:LIVIAM>2.0.CO;2

Polyakov, I.V. and Johnson, M.A., 2000. Arctic decadal and interdecadal variability. *Geophysical Research Letters*, 27, 4097–4100. doi:10.1029/2000GL011909

Przybylak, R., Vizi, Z., and Wyszynski, P., 2010. Air temperature changes in the Arctic from 1801 to 1920. *International Journal of Climatology*, 30, 791–812. doi:10.1002/joc.1918

Rayner, N.A., *et al*., 2003. Global analyses of sea surface temperature, sea ice, and night marine air temperature since the late nineteenth century. *Journal of Geophysical Research*, 108 (D), 4407. doi:10.1029/2002JD002670

Rudels, B., 2016. Arctic Ocean stability: the effects of local cooling, oceanic heat transport, freshwater input, and sea ice melt with special emphasis on the Nansen Basin. *Journal of Geophysical Research*, 121, 4450–4473. doi:10.1002/2015JC011045

Semenov, V.A., 2014. Role of sea ice in formation of wintertime Arctic temperature anomalies. *Izvestiya, Atmospheric and Oceanic Physics*, 50, 343–349. doi:10.1134/S0001433814040215

Semenov, V.A. and Bengtsson, L., 2003. Modes of the wintertime Arctic temperature variability. *Geophysical Research Letters*, 30, 1781. doi:10.1029/2003GL017112

Semenov, V.A. and Latif, M., 2012. The early twentieth century warming and winter Arctic sea ice. *The Cryosphere*, 6, 1231–1237. doi:10.5194/tc-6-1231-2012

Serreze, M.C., *et al*., 2006. The large-scale freshwater cycle of the Arctic. *Journal of Geophysical Research*, 111, C11010. doi:10.1029/2005JC003424

Soon, W., Connolly, R., and Connolly, M., 2015. Re-evaluating the role of solar variability on Northern Hemisphere temperature trends since the 19th century. *Earth-Science Reviews*, 150, 409–452. doi:10.1016/j.earscirev.2015.08.010

Stroeve, J.C., *et al*., 2012. Trends in Arctic sea ice extent from CMIP5, CMIP3 and observations. *Geophysical Research Letters*, 39, L16502. doi:10.1029/2012GL052676

Suo, L., *et al*., 2013. External forcing of the early 20th century Arctic warming. *Tellus A*, 65, 20578. doi:10.3402/tellusa.v65i0.20578

Tilling, R.L., *et al*., 2015. Increased Arctic sea ice volume after anomalously low melting in 2013. *Nature Geoscience*, 8, 643–646. doi:10.1038/NGEO2489

Titchner, H.A. and Rayner, N.A., 2014. The met office hadley centre sea ice and sea surface temperature data set, version 2: 1. Sea ice concentrations. *Journal of Geophysical Research Atmospheres*, 119, 2864–2889. doi:10.1002/2013JD020316

Vihma, T., 2014. Effects of Arctic sea ice decline on weather and climate: a review. *Surveys in Geophysics*, 35, 1175–1214. doi:10.1007/s10712-014-9284-0

Vinje, T., 2001. Anomalies and trends of sea-ice extent and atmospheric circulation in the Nordic Seas during the period 1864-1998. *Journal of Climate*, 14, 255–267. doi:10.1175/1520-0442(2001)014<0255:AATOSI>2.0.CO;2

Wake, B., 2016. Arctic precipitation. *Nature Climate Change*, 6, 127. doi:10.1038/nclimate2931

Walsh, J.E. and Chapman, W.L., 2001. 20th-century sea-ice variations from observational data. *Annals of Glaciology*, 33, 444–448. doi:10.3189/172756401781818671

Walsh, J.E., Chapman, W.L., and Fetterer, F., 2015 (updated 2016). *Gridded monthly sea ice extent and concentration, 1850 onwards, Version 1.1*. Boulder, CO: National Snow and Ice Data Center. Digital media. doi:10.7265/N5833PZ5

Walsh, J.E., *et al*., 2017. A database for depicting Arctic sea ice variations back to 1850. *Geographical Review*, 107, 89–107. doi:10.1111/j.1931-0846.2016.12195.x

Walsh, J.E. and Johnson, C.M., 1979. An analysis of Arctic sea ice fluctuations, 1953-77. *Journal of Physical Oceanography*, 9, 580–591. doi:10.1175/1520-0485(1979)009<0580:AAOASI>2.0.CO;2

Weatherly, J.W., 2004. Sensitivity of Antarctic precipitation to sea ice concentrations in a general circulation model. *Journal of Climate*, 17, 3214–3223. doi:10.1175/1520-0442(2004)017<3214:SOAPTS>2.0.CO%3B2

Wood, K.R. and Overland, J.E., 2010. Early 20th century Arctic warming in retrospect. *International Journal of Climatology*, 30, 1269–1279. doi:10.1002/joc.1973

Yamanouchi, T., 2011. Early 20th century warming in the Arctic: a review. *Polar Science*, 5, 53–71. doi:10.1016/j.polar.2010.10.002

Zakharov, V.F., 1997. Sea ice in the climate system: a Russian view. *NSIDC Special Report 16*. Boulder, CO, National Snow and Ice Data Center. Available from: https://nsidc.org/pubs/special/16/NSIDC-special-report-16.pdf [Accessed 14 January 2016]